OKLAHOMA GEOLOGY

Oklahoma
Geological
Survey

Vol. 61, No. 2 Summer 2001

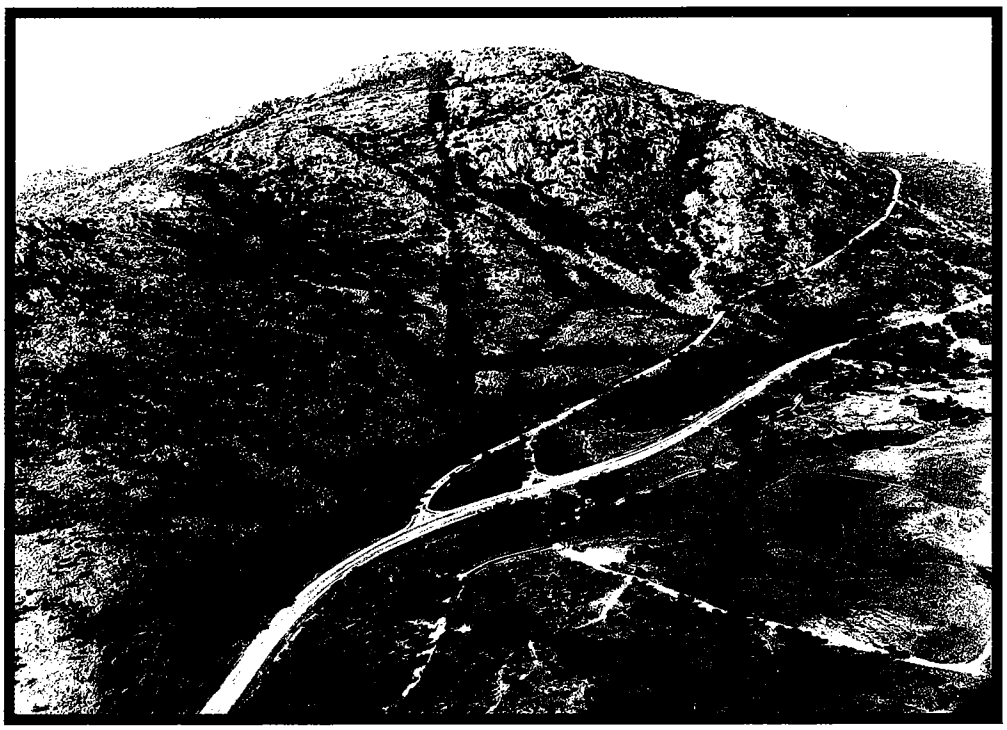

Featuring:

- *Mechanical properties of the Mount Scott Granite*
- *Oklahoma earthquakes, 2000*

on the cover

Mount Scott, Wichita Mountains, Oklahoma

It is appropriate to feature Mount Scott on the cover as the mountain is composed mostly of Mount Scott Granite, whose mechanical rock properties have been newly determined and are reported in this issue in the article beginning on p. 28. The Mount Scott Granite was defined by Merritt in 1965 from what had previously been mapped in the eastern Wichitas as Lugert Granite. Merritt used two type localities to define the Mount Scott Granite. One was Mount Scott, itself, and the other was the Ira Smith Quarry, some 14 mi to the west. A hole drilled in 1993 near that quarry provided the rock core from which samples were taken for the laboratory study.

Mount Scott Granite is the most widespread of the mapped granites in the Wichita Mountains. It crops out over a distance of some 34 mi, from the very first granite outcrops along Oklahoma State Highway 49 west of Interstate 44 to outcrops in the vicinity of Lake Tom Steed dam near Mountain Park. Mount Scott Granite is a sheet granite whose basal contact with underlying gabbroic rocks is distinctively displayed in the Mount Scott–Mount Sheridan and Cutthroat Gap areas (Fig. 1). Mount Scott Granite caps all the higher elevations in the eastern Wichitas, meaning it is relatively more resistant to erosion than surrounding rocks, a fact consistent with the high strength found in the laboratory measurements. Across its outcrop area, this granite has a very uniform chemistry and mineralogy; variations in its texture are minor. (See Fig. 2 for an example of one of the common textural types.)

Mount Scott, although not the highest in elevation in the Wichitas, does have the greatest relief (vertical distance from its base to its top) of any of the peaks. The whole vertical extent of Mount Scott on the south side (cover photo) is made up of Mount Scott Granite. On the north, the upper two-thirds of the peak is granite and the lower third is a gabbroic rock (Fig. 1). Thus, the highway up the mountain is always in Mount Scott Granite. The famous boulder stream, which the road crosses just as it begins its ascent, can be nicely seen in the cover photo. The mass of boulders in this stream originated as spheroidally weathered corestones, which then accumulated along one of the ravines weathered out along a major fracture zone.

Mount Scott Granite has a radiometrically measured age of 534 ± 1.5 million years, which makes it Early Cambrian. This age is the rock's crystallization/emplacement age—the age when the granitic magma rose to its emplacment position in the crust and then crystallized. However, the age of the "mountain" (meaning its topography) is about 280 million years, which means that it was eroded and carved into its present shape in the Early Permian. This topographic shape (the "mountain"), the rest of the Wichitas, and the Slick Hills were then buried in muds and silts carried by streams flowing westerly from the Ouachita and Ozark regions. These sediments became the Permian "redbeds" that are now being eroded away, uncovering and revealing the previously buried mountain range.

Reference Cited

Merritt, C. A., 1965, Mt. Scott Granite, Wichita Mountains, Oklahoma: Oklahoma Geology Notes, v. 26, p. 211–213.

M. Charles Gilbert
School of Geology and Geophysics
University of Oklahoma

Figure 1. This view of Mount Scott is from the west-northwest; it was taken just east of Medicine Park in the hills near Mount Cummins. The very pronounced tree line marks the base of the Mount Scott Granite as it contacts the underlying Mount Sheridan Gabbro. The gabbro's composition—much richer in calcium, magnesium, and iron than the granite—is more favorable to the growth of trees. This contact can be followed from Mount Scott westerly along the north faces of the peaks past Mount Sheridan toward Saddle Mountain.

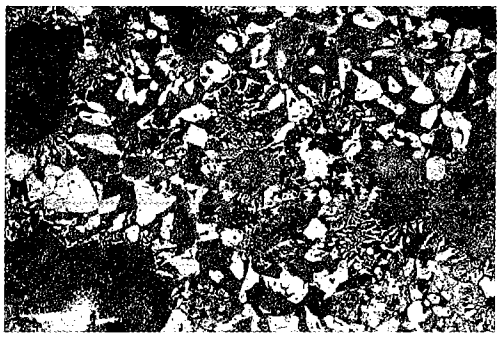

Figure 2. This photomicrograph (about 15 × 22 mm) shows some of the typical texture of the Mount Scott Granite: relatively small but variable grain size with intricately interlocking crystals. This texture presumably explains the high strength of the Mount Scott Granite. The white areas are the mineral quartz and the gray areas are feldspar. The darker, larger, gray ovoid crystals are early crystallizing feldspars that originated at some depth below the intrusion level. These ovoid feldspars have rapakivi texture (zoned with a sodium-rich outside layer) and are diagnostic of the Mount Scott Granite. The small bunches of stringy, tightly intergrown quartz and feldspar form what is called granophyric texture. This texture commonly indicates rapid cooling after the granitic magma is in its emplacement position. The black minerals are magnetite, amphibole, or biotite.

Oklahoma
Geological Survey

CHARLES J. MANKIN
Director

OKLAHOMA GEOLOGY NOTES

EDITORIAL STAFF

Christie Cooper
Managing Editor

Frances Young
Technical Editor

CARTOGRAPHIC STAFF

T. Wayne Furr
Manager

James H. Anderson
Cartographic Technician

OKLAHOMA GEOLOGY NOTES, ISSN 0030-1736, is published quarterly by the Oklahoma Geological Survey. It contains short technical articles, mineral-industry and petroleum news and statistics, abstracts, notices of new publications, and announcements of general pertinence to Oklahoma geology. Single copies, $1.50; yearly subscription, $6. Send subscription orders to the Survey at 100 E. Boyd, Room N-131, Norman, OK 73019.

EDITORIAL MATTER: Short articles on aspects of Oklahoma geology are welcome from contributors; please direct questions or requests for general guidelines to the *NOTES* editor at the address above.

This publication, printed by the Oklahoma Geological Survey, Norman, Oklahoma, is issued by the Oklahoma Geological Survey as authorized by Title 70, Oklahoma Statutes 1981, Section 3310, and Title 74, Oklahoma Statutes 1981, Sections 231–238. 1,500 copies have been prepared for distribution at a cost of $2,176 to the taxpayers of the State of Oklahoma. Copies have been deposited with the Publications Clearinghouse of the Oklahoma Department of Libraries.

OKLAHOMA GEOLOGY

Vol. 61, No. 2 Summer 2001

Mechanical Properties of the Mount Scott Granite, Wichita Mountains, Oklahoma

Oded Katz[1,2], M. Charles Gilbert[3], Ze'ev Reches[1], and J-C. Roegiers[4]

ABSTRACT.—The mechanical rock properties of the Mount Scott Granite, exposed in the Wichita Mountains, southern Oklahoma, were examined experimentally in the Rock Mechanics Institute of the University of Oklahoma, Norman. The core samples tested were from a depth of ~50 m.

Compressional-wave velocity is 4.8 ± 0.2 km/sec. The differential stress at failure increases with the confining pressure (compression is designated with a minus sign): differential stress at failure is −219 ± 25 MPa at −0.1 MPa confining pressure and −734 ± 11 MPa at −66 MPa, the maximum confining pressure tested. Young's modulus increases slightly with increasing confining pressure: it is 75.2 GPa at −0.1 MPa confining pressure and 82.0 ± 0.9 GPa at −66 MPa confining pressure. Poisson's ratio is highest (0.26–0.31) at low confining pressure; with increasing confining pressure, it decreases slightly to ~0.21. The engineering rock mass rating (RMR) of the Mount Scott Granite (at a depth of ~50 m) is "very good rock."

INTRODUCTION

The Mount Scott Granite is exposed in the Wichita Mountains, southwestern Oklahoma (Fig. 1). The Wichita Mountains are a fault-bounded, elevated portion of the Wichita igneous province, a zone of Cambrian igneous activity that trends northwest–southeast (Gilbert, 1982). This igneous province is compositionally stratified: mafic gabbros are overlain by silicic rhyolites and granites. The Mount Scott Granite intruded and spread out laterally along the rhyolite-gabbro contact (Hogan and Gilbert, 1997). The Mount Scott Granite is a fine- to medium-grained rock, which has a porphyritic texture with ovoid anorthoclase phenocrysts set in a variably granophyric matrix of alkali feldspar and quartz. Granophyre is rare to absent in the drill core (Price and others, 1996). Minor and accessory minerals typically comprise <5 modal% and include ferro-edenitic hornblende, Fe-rich biotite, titaniferous magnetite, ilmenite, titanite, zircon, apatite, and fluorite.

The mechanical properties and engineering classifications of the Mount Scott Granite are reported here as part of an ongoing investigation of brittle failure. The experimental work was conducted at the Rock Mechanics Institute of the University of Oklahoma, Norman. The material used in this study was from a 4.54-cm-diameter drill core obtained from an 87.5-m-deep hole near the old Ira Smith Quarry on the Jim Snell ranch (NE¼SE¼SW¼SE¼ sec. 4, T. 3 N., R.15 W.). Compositional, mineralogical, and other physical data of this core, as well as its geologic setting, are described by Price and others (1998). The samples tested in this study are from a depth of ~50 m, where minerals are unaltered and the rock mass is significantly less fractured than at the surface (Price and others, 1998).

[1]Institute of Earth Sciences, Hebrew University, Jerusalem, Israel.
[2]Geological Survey of Israel, Jerusalem, Israel.
[3]School of Geology and Geophysics, University of Oklahoma, Norman.
[4]School of Petroleum and Geological Engineering, University of Oklahoma, Norman.

EXPERIMENTAL PROCEDURES

Seismic Wave Velocity

Compressional-wave and shear-wave velocities were measured parallel to the original vertical axes in three granite cylinders (diameters, 2.54 cm; lengths, 3 cm), using a seismic analyzer (SBEL model SA2008) with 1 MHz transducers. The ends of the samples were ground to form two parallel surfaces (perpendicularity, 0.005 radians), which were coupled to the transducers using vacuum grease. The transducers were aligned inside a polycarbonate tube and put into an axial load frame. The velocities were measured under an axial load of −10 kN.

Mechanical Properties

Uniaxial, as well as triaxial, compression tests were performed on samples of the Mount Scott Granite. (Compression is designated with a minus sign.) Sample cylinders, 2.54 cm in diameter, were drilled from the field core. The length-to-diameter ratio of each sample was ~2.0; perpendicularity was 0.005 radians. Samples were placed between axial end pieces made of steel and then jacketed in heat-shrink plastic tubing (Fig. 2). The jacketed samples were placed inside a −69 MPa pressure vessel (SBEL model RC 10). Axial load was supplied by a stiff (9×10^9 N/m^2), servo-controlled hydraulic load frame (MTS model 315) with a −2669 kN actuator. Stroke and confining pressure were controlled using microprofilers (MTS model 458.91). Load was monitored using an internal load cell (located in the lower part of the load frame). Axial

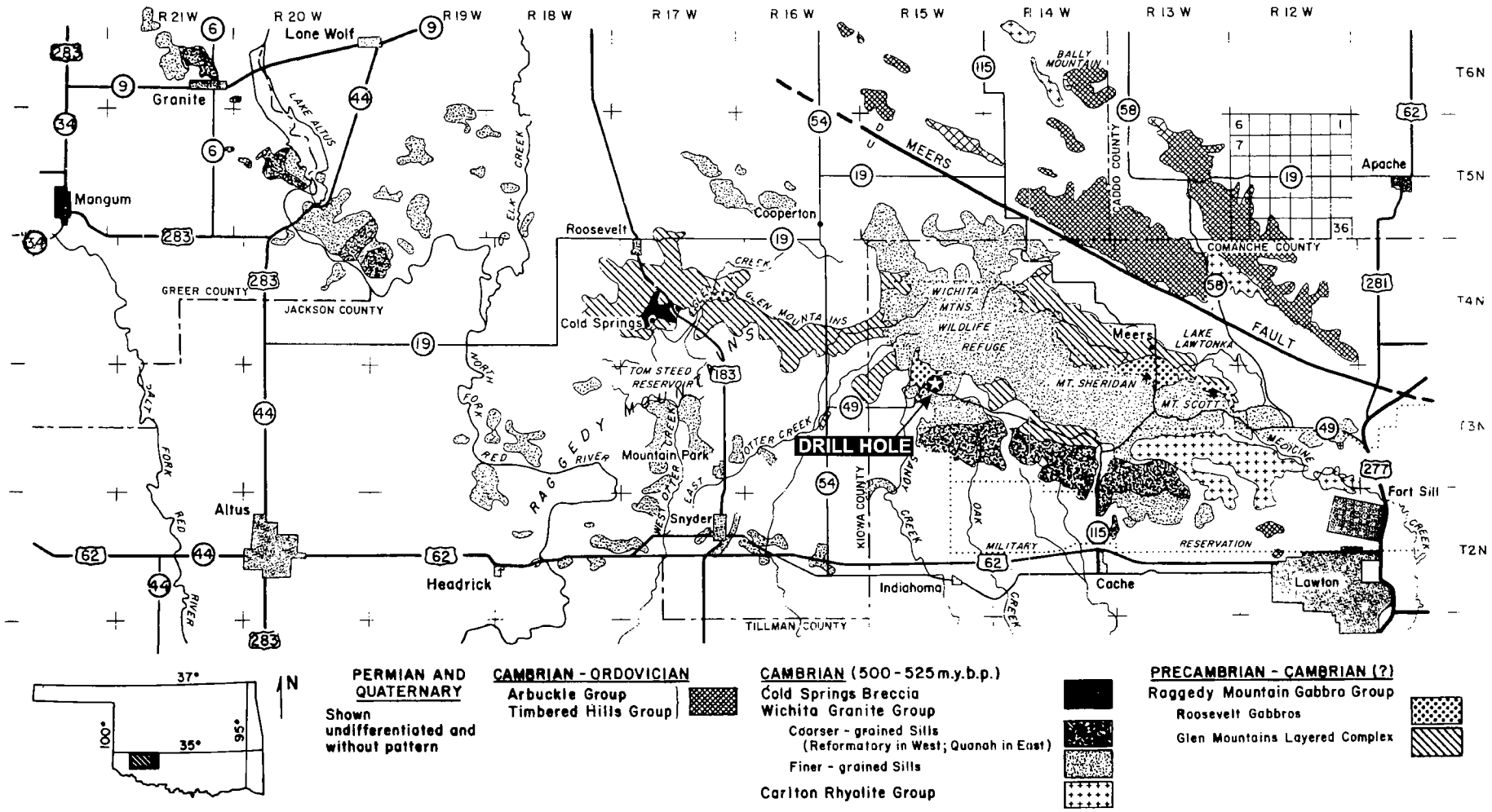

Figure 1. Location map for the sampling site (NE¼SE¼SW¼SE¼ sec. 4, T. 3 N., R. 15 W.) of the Mount Scott Granite (adapted from Powell and others, 1980). The grid shows the section (square mile) numbering system applied within a given township and range.

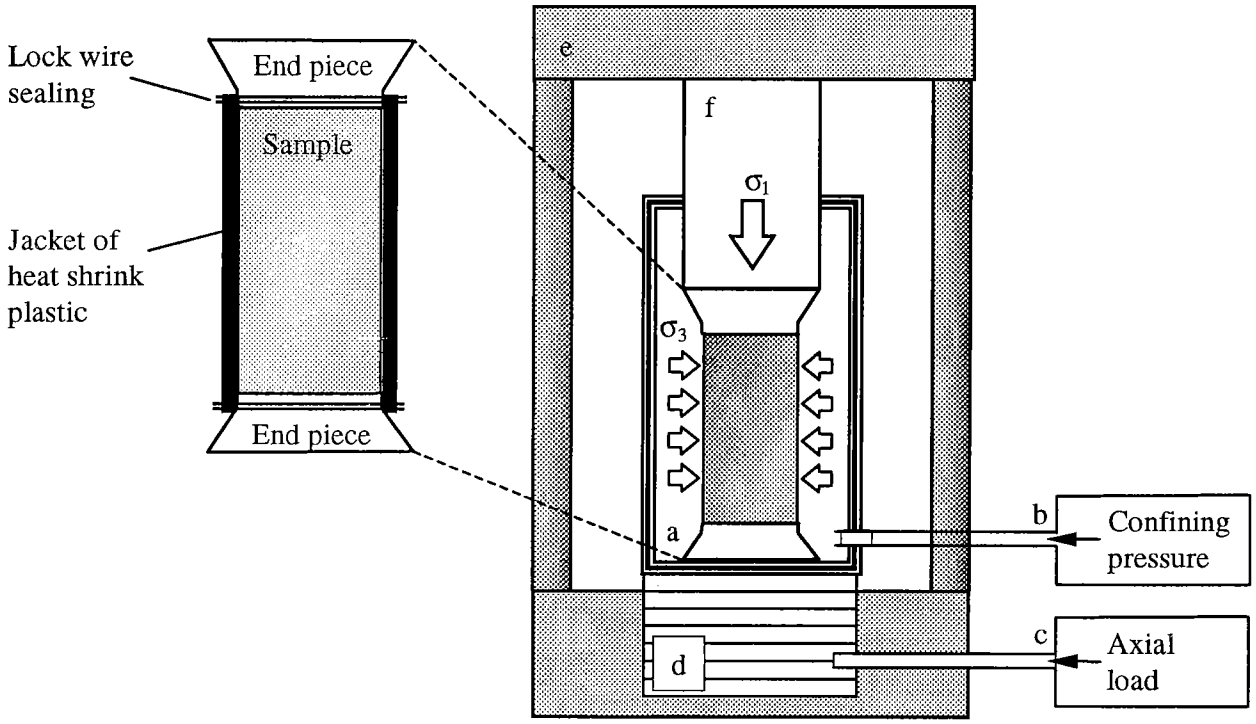

Figure 2. Experimental setup: Each sample (left side of the figure) was placed between steel axial-end pieces, which were used to adapt the sample to the machine. Heat-shrink plastic tubing (PTE) jacketed the sample and overlapped onto the axial-end pieces; double loops of stainless steel lock wire were attached to clamp and seal the jacket to the end pieces. The sample was then placed inside a pressure vessel (a, right side of the figure) that was filled with hydraulic oil. Confining pressure (σ_3) was applied to the sample by increasing the pressure in the vessel using a hydraulic pump (b). A second hydraulic system (pump [c] and piston [d]) applied axial stress (σ_1) to the sample: the piston pushed the pressure vessel (a) upward against the load frame (e), and the axial stress was applied through a steel rod (f).

displacement in the sample was monitored using two Schaevitz linear velocity displacement transducers located across the core. Lateral displacement in the sample was monitored using a chain extensometer (MTS model 632.92B-05) attached at the middle of the long dimension of the sample. The stroke rate during the tests was a constant 1×10^{-5} sec^{-1}.

All specimens were loaded until failure, with the exception of one (Test 11, Table 1), which was loaded to 96% of its strength (that is, 96% of the average strength at failure of the other two samples tested at the same confining pressure). Confining pressures ranged from –0.1 to –66 MPa, the last corresponding to a depth of ~2.5 km. Density was calculated using the oven-dry weights and dimensions of the samples. Young's modulus (E) and Poisson's ratio (v) were calculated before the onset of dilation in the samples (i.e., using the linear part of the curve for differential stress vs. volumetric strain). The fault angle (θ), between the direction of the shear fracture and the direction of σ_3 (the minimum compressive stress) was measured on each sample.

RESULTS

Seismic Wave Velocity

Compressional-wave and shear-wave velocities were evaluated in three samples, as described in the section on experimental procedures, above. The average compressional-wave velocity is 4.8 ± 0.2 km/sec. The shear-wave velocity, which is not well constrained due to technical problems, is 0.49–0.62 of the compressional-wave velocity.

Mechanical Properties

Uniaxial compressive tests (confining pressure = –0.1 MPa) were performed on three samples of the Mount Scott Granite and triaxial tests were performed on 10 samples. The results are shown in Table 1 and Figure 3. The ultimate strength (differential stress, $\sigma_1 - \sigma_3$, at failure), Young's modulus, and Poisson's ratio as a function of the confining pressure (σ_3) are shown in Figure 4. The differential stress at failure increases with the confining pressure: it is –219 ± 25 MPa at –0.1 MPa confining pressure and –734 ± 11 MPa at –66 MPa, the maximum confining pressure tested. Young's modulus increases slightly with confining pressure: it is 75.2 GPa at –0.1 MPa confining pressure and 82.0 ± 0.9 GPa at –66 MPa confining pressure. (Test 3 [Table 1] gave a very high modulus; it is plotted in Figure 4B, but it was not used in the analysis). Poisson's ratio is highest (0.26–0.31) at low confining pressure (–0.1 to –14 MPa); then it decreases slightly to ~0.21 and shows little variation with increasing confining pressure.

The fault pattern at failure changed with increasing confining pressure (Fig. 5). Axial splitting with few major fractures and numerous minor cracks developed in uniaxial tests. Major faults characterized failure when confining pressure was applied. Under the low confining pressures of –14 to –28 MPa, fracturing patterns were diffuse: a few major

TABLE 1. — Summary of Results of Experimental Tests on the Mount Scott Granite

Test no.	Sample length[a] (cm)	Sample density[a] (kg/m³)	Confining pressure (σ_3) (MPa)	Differential stress (σ_1–σ_3) at failure (MPa)	Young's modulus (E)[b] (GPa)	Poisson's ratio (ν)[b]	Fault angle (θ)[c] (degrees)
2	5.4	2,660	–0.1	–192	75.2	0.26	Axial splitting
2b	5.2	2,673	–0.1	–223	75.2	0.25	Axial splitting
3	5.0	No data	–0.1	–243	89.6	0.31	Axial splitting
4	5.1	2,640	–7	–376	75.8	0.20	71
5	5.8	2,623	–14	–433	76.5	0.24	72
6	5.3	2,648	–14	–392	76.0	0.27	72
7	5.4	No data	–28	–511	77.1	0.21	70
10	5.2	2,659	–28	–491	78.6	0.21	74
11	5.3	2,643	–28	No failure	76.6	0.22	—
8	5.3	2,641	–41	–627	79.4	0.22	69
9	6.1	2,638	–41	–622	78.1	0.21	75
12	5.1	2,633	–66	–742	81.4	0.23	73
13	5.0	2,634	–66	–726	82.7	0.20	68

[a]Calculated using the oven-dry weights and dimensions of the core samples.
[b]Calculated before the onset of dilation.
[c]Measured on the core samples.

faults were accompanied by numerous small cracks. Under the higher confining pressures of –41 to –66 MPa, fewer small faults and cracks accompanied a single major fault.

The compressive strength of the Mount Scott Granite was evaluated from the Mohr-Coulomb failure envelope (Fig. 6). The failure strength is represented by two material properties: cohesion, C, and the angle of internal friction, ϕ,

(1) $$\tau = C + \sigma_n \tan\phi$$

where τ and σ_n are the shear stress and the normal stress, respectively, on the fault plane at failure. Two methods, both following Brady and Brown (1985), were used to evaluate C and ϕ. The first uses the linear relation between the maximum compressive stress at failure, maximum σ_1, and the confining pressure, σ_3,

(2) $$C = [\sigma_c(1 - \sin\phi)]/2\cos\phi$$

(3) $$\sin\phi = (\tan\psi - 1)/(\tan\psi + 1)$$

where σ_c and ψ are the intercept and the slope, respectively, of the linear regression line fitted to the experimental data (Fig. 6A). The values for C and ϕ calculated from equations 2–3 can be used in equation 1 to calculate the failure envelope in the shear stress vs. normal stress space (black line, Fig. 6B).

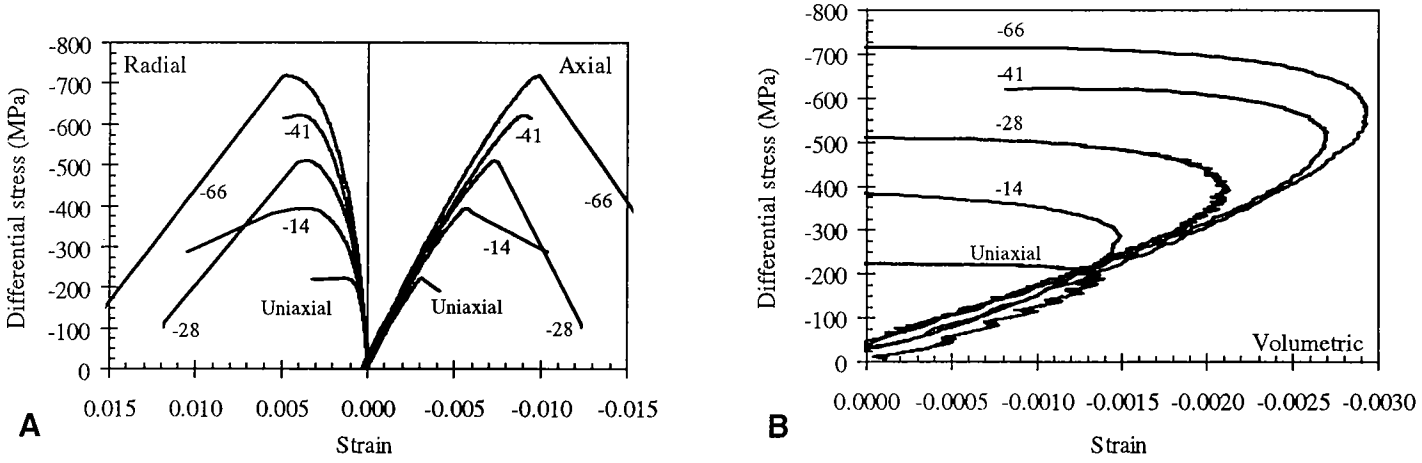

Figure 3. Results of selected compression tests showing the differential-stress–strain curves. (Compression is designated with a minus sign.) The confining pressure (in MPa) for each test is shown near its curve, and curves for uniaxial tests are so labeled. *A*—Axial and radial strains. *B*—Volumetric strain.

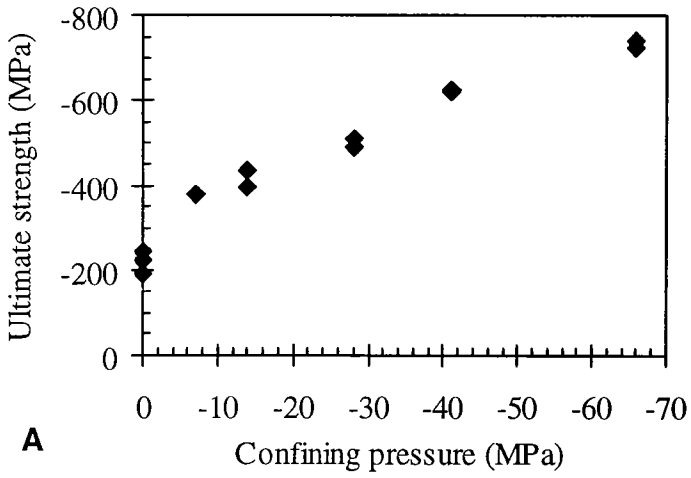

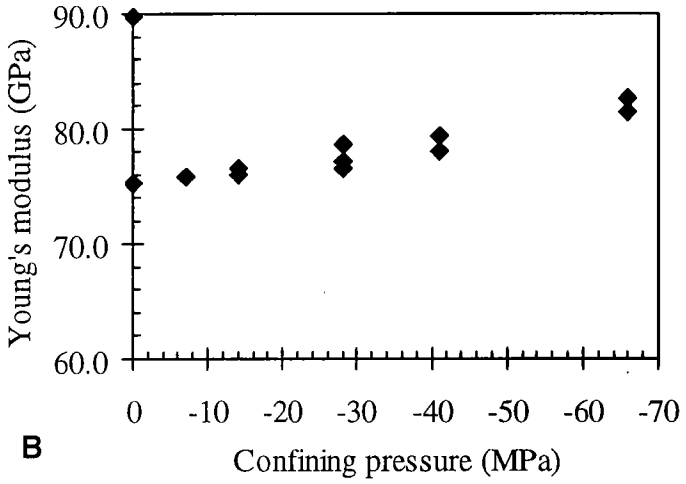

Figure 4 *(above and right)*. Mechanical properties of the Mount Scott Granite as functions of the confining pressure, σ_3 (compression is designated with a minus sign). *A*—Ultimate strength (differential stress, $\sigma_1 - \sigma_3$, at failure). *B*—Young's modulus. *C*—Poisson's ratio.

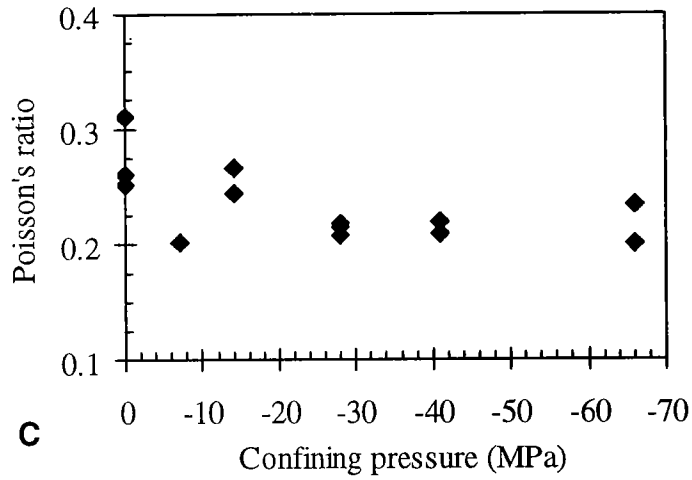

Figure 5 *(below)*. Fault patterns at failure of the Mount Scott Granite under different experimental conditions. The fractures are identified by doubled arrows. *A*—Axial splitting developed in uniaxial tests. *B*—Under relatively low confining pressure (–14 to –28 MPa), the fracturing patterns were rather diffuse: a few major faults were accompanied by numerous small cracks. *C*—Under high confining pressure (–41 to –66 MPa), fewer small faults and cracks accompanied a single major fault.

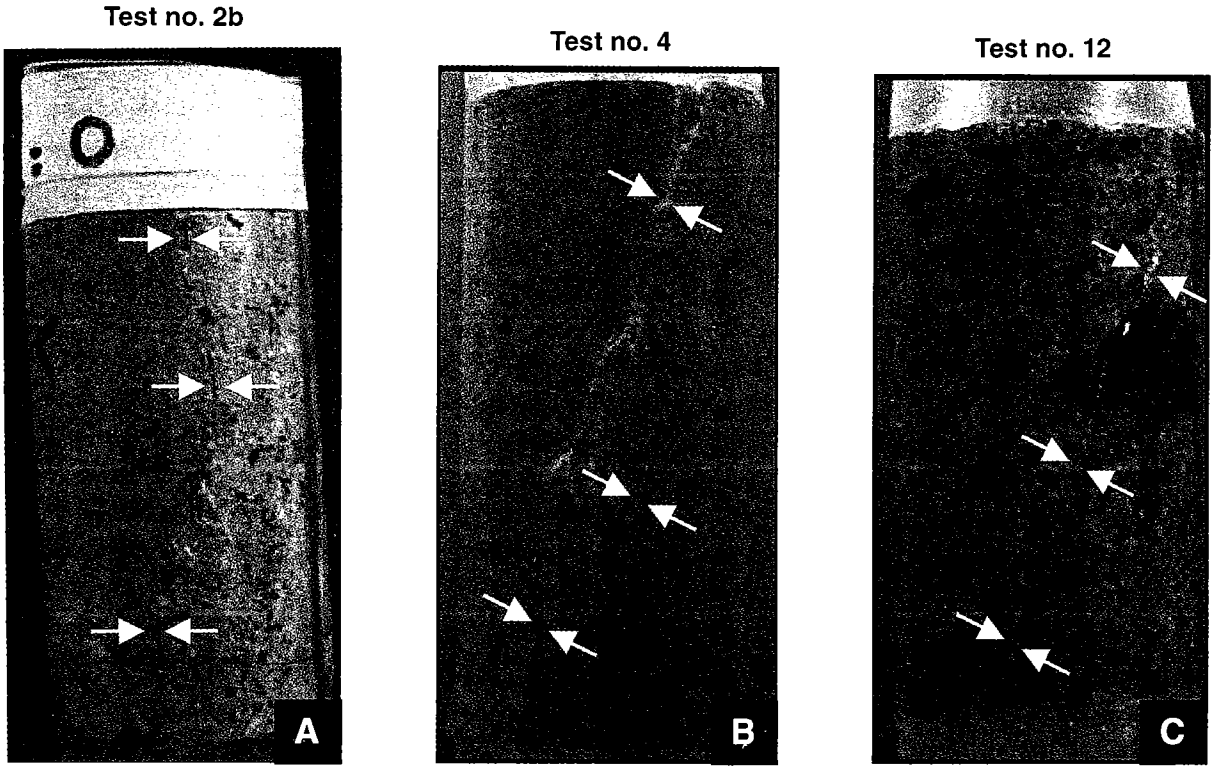

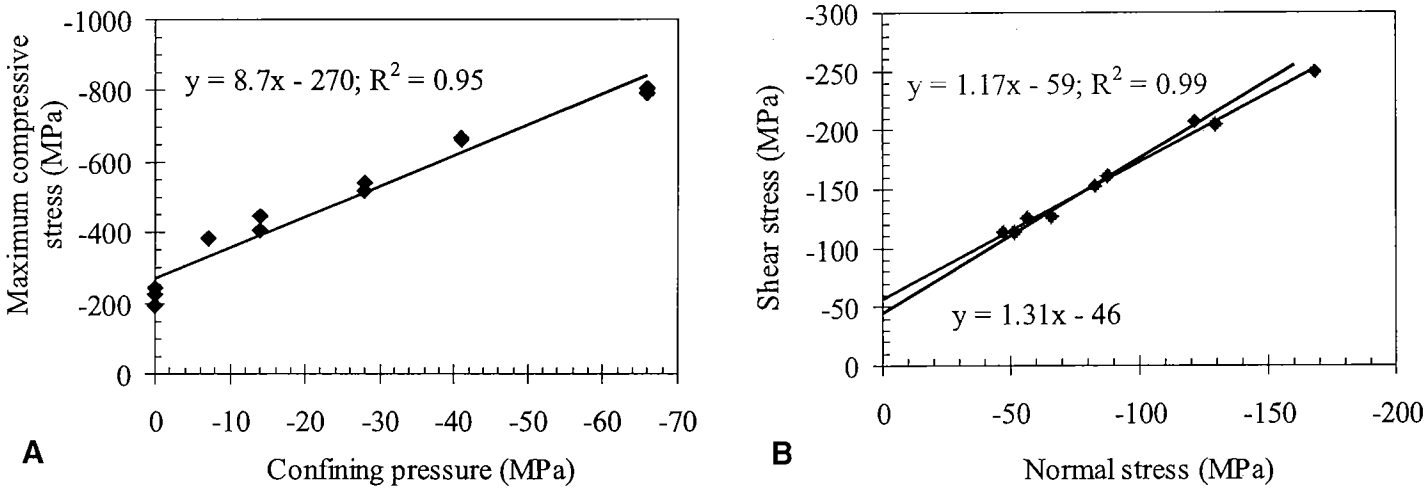

Figure 6. Failure envelope of the Mount Scott Granite. *A*—Plot of maximum compressive stress (σ_1 at failure) as a function of the confining pressure, showing the Mohr-Coulomb failure envelope. *B*—Plot of shear stress vs. normal stress showing two calculations of the Mohr-Coulomb failure envelope. The black line is calculated using equations 2–3 (discussed in the text). The orange line is calculated using equations 4–5 (discussed in the text). Note: Because axial splitting rather than shear fractures formed in uniaxial tests (confining pressure = 0), data from those tests are not included.

The second method for evaluating C and ϕ uses the linear regression between the normal stress (σ_n) and the shear stress (τ) of equation 1, according to relations:

(4) $$\sigma_n = \tfrac{1}{2}(\sigma_1 + \sigma_3) + \tfrac{1}{2}(\sigma_1 - \sigma_3)\cos 2\theta$$

(5) $$\tau = \tfrac{1}{2}(\sigma_1 - \sigma_3)\sin 2\theta$$

where θ is the measured angle of the fault plane with respect to the direction of σ_3 (least compressive stress). The cohesion, C, and angle of internal friction, ϕ, are the intercept and the slope, respectively, of the linear regression line fitted to the points calculated from equations 4–5 (orange diamonds and line, Fig. 6B).

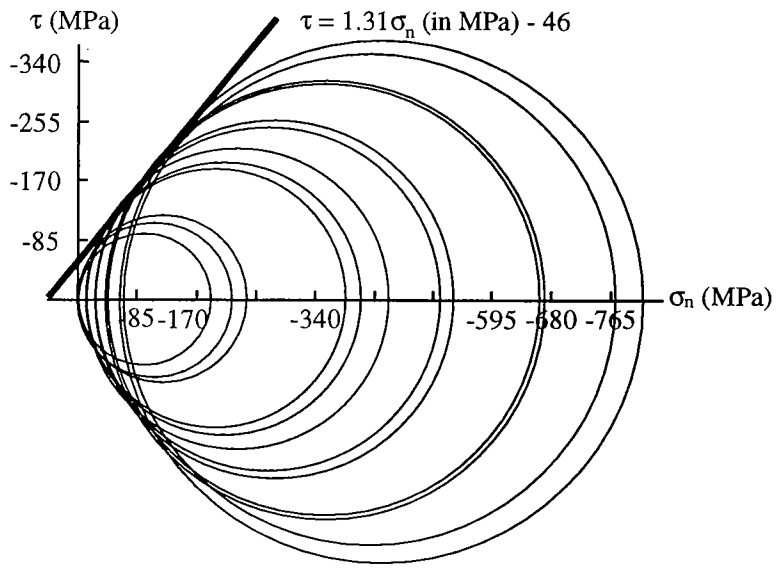

Figure 7. Mohr diagram of the Mount Scott Granite. Circles are according to the experimental data; the failure envelope is calculated using equations 2–3 (discussed in the text).

For the Mount Scott Granite, C = –46 MPa and ϕ = 53° (black line, Fig. 6B), according to the first method (equations 2–3), where σ_c = –270 MPa and ψ = 8.7 (Fig 6A); according to the second method (equations 4–5), C = –59 MPa and ϕ = 49° (orange line, Fig 6B). Figure 7 shows the Mohr diagram. Equations 2–3 are chosen to calculate the failure envelope in Figure 7 because they use only experimental results. (The values for θ used in equations 4–5 are measurements, which could introduce errors.)

The mechanical properties of the Mount Scott Granite are compared to those of a few other granitic rocks known from the rock mechanics literature (Table 2). For the Mount Scott Granite, the values for ultimate strength (differential stress, $\sigma_1 - \sigma_3$, at failure), compressive-wave velocity, Young's modulus, and Poisson's ratio are high relative to those values for the other granites.

ENGINEERING ROCK MASS CLASSIFICATION

According to standards in Deere and Miller (1966), the Mount Scott Granite (at a depth of ~50 m) has very high strength (type A: uniaxial compressive strength higher than –215 MPa) and an average modulus ratio (the ratio of Young's modulus to the uniaxial compressive strength is between –200 and –500). According to the engineering rock mass rating (RMR) of Bieniawski (1973, 1989), the Mount Scott Granite (at a depth of ~50 m) is "very good rock," and it is expected to have cohesion of more than –0.3 MPa and an angle of internal friction of more than 45° (shown experimentally). At a depth of ~50 m, the Mount Scott Granite could sustain large (meters wide), unsupported underground excavation for long periods of time.

TABLE 2. — Comparison of the Mechanical Rock Properties of the Mount Scott Granite with Those of Selected Granites

	Origin	Differential stress (σ_1–σ_3) at failure (MPa)	Compressional wave velocity (km/sec)	Young's modulus (E) (GPa)	Poisson's ratio (v)
Westerly Granite[a]	Rhode Island	–230		50	0.28
Barre Granite[b]	Vermont	–229	3.4	30	
Mount Scott Granite	Oklahoma	–219	4.8	75	0.26
Grand Junction Granite[b]	Colorado	–174	3.17	27	0.19
Nevada test site granite[b]	Nevada	–141		74	0.22

[a]Values for properties from Brace and others (1966).
[b]Values for properties from Carmichael (1989).

SUMMARY

The wave velocities and mechanical rock properties of the Mount Scott Granite at a depth of ~50 m were investigated. Compressional-wave velocity is 4.8 ± 0.2 km/sec; shear-wave velocity is 0.49–0.62 of the compressional-wave velocity. The uniaxial compressive strength is –219 ± 25 MPa. Following two methods of Brady and Brown (1985), the Mohr-Coulomb failure envelope is given by $\tau = -46 + 1.31\sigma_n$ (in MPa), calculated using equations 2–3, above, and by $\tau = -59 + 1.17\sigma_n$ (in MPa), calculated using equations 4–5, above. Young's modulus and Poisson's ratio under uniaxial conditions are 75.2 GPa and 0.26, respectively. Experimental procedures were performed on samples of the Mount Scott Granite from a depth of ~50 m. It is likely that the rock strength would be somewhat lower at the surface because of mineral alteration and increased fracturing.

The Mount Scott Granite was compared to a few other granitic rocks. It has high values for ultimate strength (differential stress, $\sigma_1 - \sigma_3$, at failure), compressive wave velocity, Young's modulus, and Poisson's ratio relative to those values for the other granites.

ACKNOWLEDGMENTS

The laboratory work was conducted at the Rock Mechanics Institute, University of Oklahoma, Norman, with the invaluable help and advice of Gene Scott and Pete Keller. The study was supported by funds from the Eberly Family Chair of M. Charles Gilbert, School of Geology and Geophysics, University of Oklahoma, Norman, as well as by the Rock Mechanics Institute. John P. Hogan provided a helpful review.

REFERENCES CITED

Bieniawski, Z. T., 1973, Engineering classification of jointed rocks masses: Transactions, South African Institution of Civil Engineering, v. 15, p. 335–344.

———— 1989, Engineering rock mass classifications: a complete manual for engineers and geologists in mining, civil, and petroleum engineering: John Wiley and Sons, New York, 251 p.

Brace W. F.; Paulding, B. W., Jr.; and Scholz, C., 1966, Dilatancy in the fracture of crystalline rocks: Journal of Geophysical Research, v. 71, p. 3939–3953.

Brady, B. H. G.; and Brown, E. T., 1985, Rock mechanics for underground mining: George Allen & Unwin, London, 527 p.

Carmichael, R. C., 1989, CRC practical handbook of physical properties of rock and minerals: CRC Press, Inc., p. 226–227.

Deere, D. U.; and Miller, R. P., 1966, Engineering classification and index properties for intact rock: University of Illinois contract AF 29(601)-6319, Technical Report AFWL-TR-65-116.

Gilbert, M. C., 1982, Geologic setting of east Wichita Mountains, with a brief discussion of unresolved problems, *in* Gilbert, M. C.; and Donovan, R. N. (eds.), Geology of the eastern Wichita Mountains, southwestern Oklahoma: Oklahoma Geological Survey Guidebook 21, p. 1–28.

Hogan, J. P.; and Gilbert, M. C., 1997, Intrusive style of A-type sheet granites in a rift environment: the southern Oklahoma aulacogen, *in* Ojakangas, R. W.; Dickas, A. B.; and Green, J. C. (eds.), Middle Proterozoic to Cambrian rifting, central North America: Geological Society of America Special Paper 312, p. 299–311.

Powell, B. N.; Gilbert, M. C.; and Fischer, J. F., 1980, Lithostratigraphic classification of basement rocks of the Wichita province, Oklahoma: Geological Society of America Bulletin, v. 91, part 1 (summary), p. 509–514, and part 2 (complete article on microfiche), p. 1875–1994.

Price, J. D.; Hogan, J. P.; and Gilbert, M. C., 1996, Rapakivi texture in the Mount Scott Granite, Wichita Mountains, Oklahoma: European Journal of Mineralogy, v. 8, p. 435–451.

Price, J. D.; Hogan, J. P.; Gilbert, M. C.; and Payne, J. D., 1998, Surface and near-surface investigation of the alteration of the Mount Scott Granite and geometry of the Sandy Creek Gabbro pluton, Hale Spring area, Wichita Mountains, Oklahoma, *in* Hogan, J. P.; and Gilbert, M. C. (eds.), Basement tectonics 12: Central North America and other regions: Proceedings of the International Conference on Basement Tectonics, v. 6, p. 79–122.

Oklahoma Earthquakes, 2000

James E. Lawson, Jr.
Oklahoma Geological Survey Observatory, Leonard

Kenneth V. Luza
Oklahoma Geological Survey

INTRODUCTION

More than 930,000 earthquakes occur throughout the world each year (Tarbuck and Lutgens, 1990). Approximately 95% of these earthquakes have a magnitude of <2.5 and are usually not felt by humans (Table 1). Only 20 earthquakes, on average, exceed a magnitude 7.0 each year. An earthquake that exceeds a magnitude 7.0 is considered to be a major earthquake and serious damage could result. (See the Catalog section, below, for a discussion of earthquake magnitude.)

Earthquakes tend to occur in belts or zones. For example, narrow belts of earthquake epicenters coincide with oceanic ridges where plates separate, such as in the mid-Atlantic and east Pacific Oceans. Earthquakes also occur where plates collide and/or slide past each other. Although most earthquakes originate at plate boundaries, a small percentage occur within plates. The New Madrid (Missosuri) earthquakes of 1811–12 are examples of large and destructive intraplate earthquakes in the United States.

The New Madrid earthquakes of 1811 and 1812 were probably the earliest historical earthquake tremors felt in what is now southeastern Oklahoma (then part of Arkansas Territory). Before Oklahoma became a state, the earliest documented earthquake occurred on October 22, 1882, probably near Fort Gibson, Indian Territory, although it cannot be located precisely (Ross, 1882; Indian Pioneer Papers, date unknown). The *Cherokee Advocate* newspaper reported that at Fort Gibson "the trembling and vibrating were so severe as to cause doors and window shutters to open and shut, hogs in pens to fall and squeal, poultry to run and hide, the tops of weeds to dip, [and] cattle to lowe" (Ross, 1882, p. 1). These observations indicate Modified Mercalli (MM)-VIII intensity effects. (See the section, below, on Distribution of Oklahoma Earthquakes for information about the MM earthquake-intensity scale.) The next documented earthquake in Oklahoma occurred near Jefferson, Grant County, on December 2, 1897 (Stover and others, 1981). The next known Oklahoma earthquake happened near Cushing, Payne County, in December 1900. This event was followed by two additional earthquakes in the same area in April 1901 (Wells, 1975).

The largest known Oklahoma earthquake (with the possible exception of the 1882 earthquake) occurred near El Reno, Canadian County, on April 9, 1952. This magnitude-5.5 (mb, Gutenberg-Richter) earthquake caused a 50-ft long crack in the State Capitol Office Building in Oklahoma City. It was felt throughout Oklahoma and in parts of seven other states. The total felt area was ~362,000 km² (Docekal, 1970; Kalb, 1964; von Hake, 1976); Des Moines, Iowa, and Austin, Texas, were at the northern and southern limits. From 1897 through 2000, 1,625 earthquakes have been located in Oklahoma.

TABLE 1. — ESTIMATED NUMBER OF WORLDWIDE EARTHQUAKES PER YEAR BY MAGNITUDE
(Modified from Tarbuck and Lutgens, 1990)

Magnitude	Estimated number per year	Earthquake effects
<2.5	>900,000	Generally not felt, but recorded
2.5–5.4	30,000	*Minor to moderate earthquakes* Often felt, but only minor damage detected
5.5–6.0	500	*Moderate earthquakes* Slight damage to structures
6.1–6.9	100	*Moderate to major earthquakes* Can be destructive in populous regions
7.0–7.9	20	*Major earthquakes* Inflict serious damage if in populous regions
≥8.0	1–2	*Great earthquakes* Produce total destruction to nearby communities

INSTRUMENTATION

A statewide network of 10 seismograph stations operated by the Oklahoma Geological Survey (OGS) was used to locate 29 earthquakes in Oklahoma for 2000 (Fig. 1). The statewide network consists of a central station (TUL/LNO), 4 radio-telemetry seismograph stations (FNO, RLO, SIO, VVO), and 4 volunteer-operated field stations (ACO, CCOK, MEO, PCO). The U.S. Geological Survey (USGS) established a seismograph station, WMOK, 19 km southwest of the OGS station at Meers (MEO). WMOK, the USGS station, does not record continuously. When triggered by moderately strong ground motion, it transmits a short segment of data to the National Earthquake Information Service in Golden, Colorado. WMOK is used mostly for distant earthquakes, although it sometimes

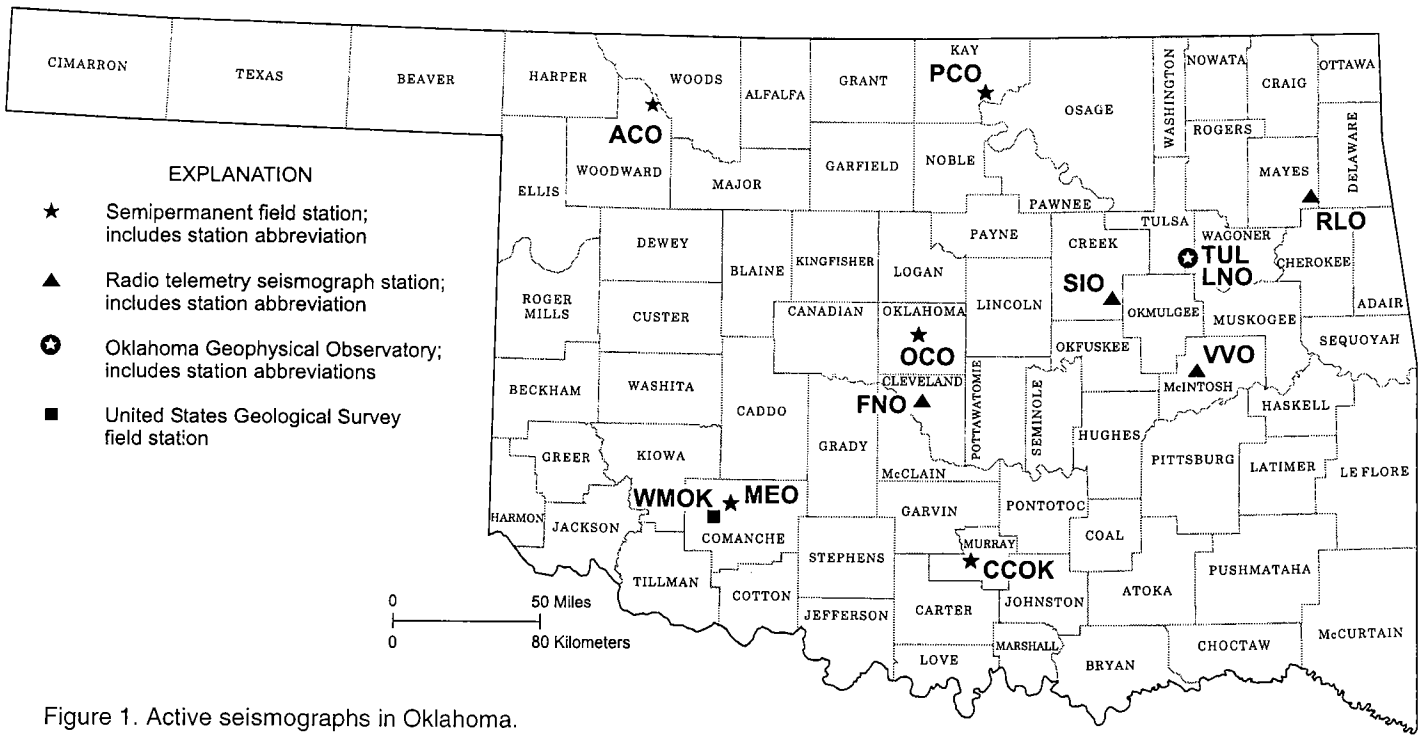

Figure 1. Active seismographs in Oklahoma.

records some of the larger Oklahoma earthquakes. Because WMOK is so near MEO, its arrival times do not improve the accuracy of location of Oklahoma earthquakes.

Central Station

The OGS Observatory station, TUL/LNO, is located ~3.2 km south of Leonard, Oklahoma, in southeastern Tulsa County. At this site, digital and analog (paper) records from all stations are analyzed to detect, identify, and locate Oklahoma earthquakes. Seismometers at the central station are located on a pier in a 4-m-deep underground walk-in vault and in a 864-m-deep borehole. The vault is designated by the abbreviation, TUL, and the borehole has the international station abbreviation, LNO. In the vault, three Baby Benioff seismometers and a 3-component Guralp CMG3-TD seismometer record vertical, north-south, and east-west ground motion. Each Baby Benioff seismometer produces signals recorded on a drum recorder that uses a heat stylus and heat sensitive paper. (The original drum recorders used light beams to record on photopaper. The drum recorders were converted to ink recording in 1978 and later to more reliable recording on heat sensitive paper.)

The Guralp CMG3-TD ultra-broadband seismometer senses everything from the solid earth tides with their μHz frequencies to the high frequencies of Oklahoma earthquakes, which may approach 100 Hz. The CMG3-TD seismometer has a Global Positioning System (GPS) time receiver and digitizers in the case. The three digitizers produce 200 samples per second each. The CMG3-TD in the vault is a temporary replacement for the similar borehole seismometer, which currently is being rebuilt under warranty at the Guralp factory in the UK. When the borehole seismometer is operating again, it will provide the 200-sample-per-second signals from the central station that are used to detect and locate earthquakes in Oklahoma.

Until May 2000, data from the Guralp seismometer and three radio-telemetry stations (RLO, VVO, and SIO) have been recorded, analyzed, and archived on a GSE digital seismic system provided by the Defense Advanced Research Projects Agnecy/Nuclear Monitoring Research Office. Signals have been digitized by a Geotech RDAS (Remote Data Acquisition System) unit at either 3,600 or 1,200 24-bit samples per second (Lawson and Luza, 2000). On May 6, 2000, the GSE system RDAS was damaged, apparently by lightning-induced power surges. It could not be reactivated with the backup circuit boards on hand, and additional boards are no longer available from the manufacturer. Therefore, the GSE system was discontinued, which left only paper drum recordings for the field telemetry stations (RLO, VVO, and SIO).

A new Guralp eight-channel rack digitizer, purchased by the OGS, was delivered on June 2, 2000. On the same day, it began recording the remote stations at 200 samples per second. Data are now digitized and recorded by Guralp SCREAM software running on a PC. These samples are assembled into time-tagged data-compressed packets and transmitted at 38,400 bits per second to the Guralp SCREAM data acquisition software. Each packet is held in a memory-ring buffer in the seismometer until SCREAM acknowledges its receipt. Any missed packet is sent again. Guralp SCREAM software, which runs on a PC, uncompresses the packets, organizes them into one-hour files on a disk, and will display one or more windows containing one or several moving traces. The windows may contain as little as one second or as much as 24 hours of ground motion. All digital data are archived on writable CD-ROMs. About two new CDs are added each week.

SCREAM sends slower packets (20 samples per second, and four samples per second) to another PC running SCREAM, and to the University of Indiana over the internet. From Indiana, the packets are sent continually or in once-per-day batches to a number of secondary schools in the United States. These slower packets lack the high frequencies characteristic of Oklahoma earthquakes but are very useful for studying teleseisms (distant earthquakes), which occur daily in the Earth's seismic belts. For distant earthquakes above magnitude 6, packages of the 20-sample-per-second, vertical, north-south, and east-west signals containing about one hour of recording are made up at the Observatory. These are sent by internet file transfer protocol to the PEPP (Princeton Earth Physics Project) database, which is used primarily by American secondary schools.

Radio Telemetry Stations

Three radio-telemetry stations, (1) at Rose Lookout (RLO) in Mayes County, (2) at the Bald Hill Ranch near Vivian (VVO) in McIntosh County, and (3) at the Jackson Ranch near Slick (SIO) in Creek County, have Geotech S-13 seismometers in shallow tank vaults. The seismic signals are amplified and used to frequency modulate an audio tone that is transmitted to Leonard with 500-mW FM transmitters at various frequencies in the 216–220-MHz band.

Oklahoma earthquake catalogs, earthquake maps, some seismograms, and related information are on the Internet at ***http://www.okgeosurvey1.gov***

Antennas on a 40-m-high tower near the OGS Observatory receive signals from the three radio-telemetry sites. These electrical signals are carried 350 m overland to the outside of the Observatory building. In a box on the outside wall, the electrical signals are converted to optical signals. The optical signals are sent through about 6 m of plastic fiber into the building, where they are converted back to electrical signals. This optical link is used to prevent wires from carrying lightning-induced surges into the building and damaging digitizers and computers.

The radio-telemetry signals are frequency-modulated audio tones. Discriminators convert the tones back into a voltage similar to the voltage produced at the field seismometer. These voltages are recorded on a 48-hour-paper-seismogram drum recorder, one recorder per station. The paper records are used mainly to backup the computer system.

The radio-telemetry signals are transmitted to three channels (one channel per station) on the Guralp rack digitizer. Each digitizer channel produces 200 samples per second. The digitizer includes a GPS (Global Positioning System) satellite receiver. The signals are assembled in memory into timed packets. The packets are transmitted to a PC running Guralp SCREAM data acquisition software.

A fourth radio-telemetry station, FNO, was installed in central Oklahoma on April 28, 1992, in Norman. The seismometer, Geotech S-13, is on a concrete pad, ~7 km northeast of Sarkeys Energy Center (the building that houses the OGS main office). A discriminator converts the audio-signal frequency fluctuations to a voltage output. The voltage-output is amplified and recorded by a Sprengnether MEQ-800 seismograph recorder (located in an OGS display case) at a trace speed of 60 mm/min.

Field Stations

Seismograms are recorded at 4 volunteer-operated seismographs (ACO, CCOK, MEO, and PCO). Each station consists of a Geotech S-13 short-period vertical-motion-sensing seismometer in a shallow tank vault, or in an abandoned mine shaft (station MEO). The seismometer signal runs through 60–600 m of cable in surface PVC conduit to the volunteer's house or other building. The volunteer has a Sprengnether MEQ-800B timing system amplifier-filter-drum recorder, which records 24 hours of seismic trace at 1 mm/min in a spiral path around the paper on the drum. A time-signal- radio receiver tuned to the National Institute of Standards and Technology and high-frequency radio station WWV is used to set the time. The volunteers mail the seismograms to the Observatory weekly (or more often, if requested). When an earthquake is felt in Oklahoma, the volunteer operators fax seismogram copies to the Observatory so that the earthquake can be located rapidly.

Station OCO, which contains equipment similar to that at the volunteer-operated stations, is at the Omniplex museum in Oklahoma City. Omniplex staff members maintain the equipment and change the seismic records daily. OGS Observatory staff help interpret the seismic data and archive the seismograms with all other Oklahoma network seismograms.

DATA PROCESSING AND ANALYSIS

Data are processed on two networked Sun Unix workstations, a SPARC20 and a SPARC 2+. All network digital and analog short-period (frequencies > ~1 Hz) and broadband seismograms are scanned for earthquakes in and near Oklahoma. The arrival times of P and S phases are recorded on a single-page form in a loose-leaf notebook. The arrivals then are entered into the SPARC20 or the SPARC 2+ using a user-friendly flexible program written in the Nawk language. The program uses the entries to write an input file with a unique file name.

From the input files, the hypocenters are located by Johannes Schweitzer's (1997) program HYPOSAT 3.2c. A Nawk program manages the input to HYPOSAT and puts the output in a single file and writes a line in an overall catalog file.

HYPOSAT must have a velocity model of the crust and top of the mantle to calculate travel times of P and S to each station from each successive hypocenter tried in the program. The nine-layer-plus-upper-mantle Chelsea model for Oklahoma, derived by Mitchell and Landisman (1971), is used exclusively for locating Oklahoma earthquakes. This model and three other Oklahoma models are outlined on the Observatory Web site at http://www.okgeosurvey1.gov/level2/geology/ok.crustal.models.html.

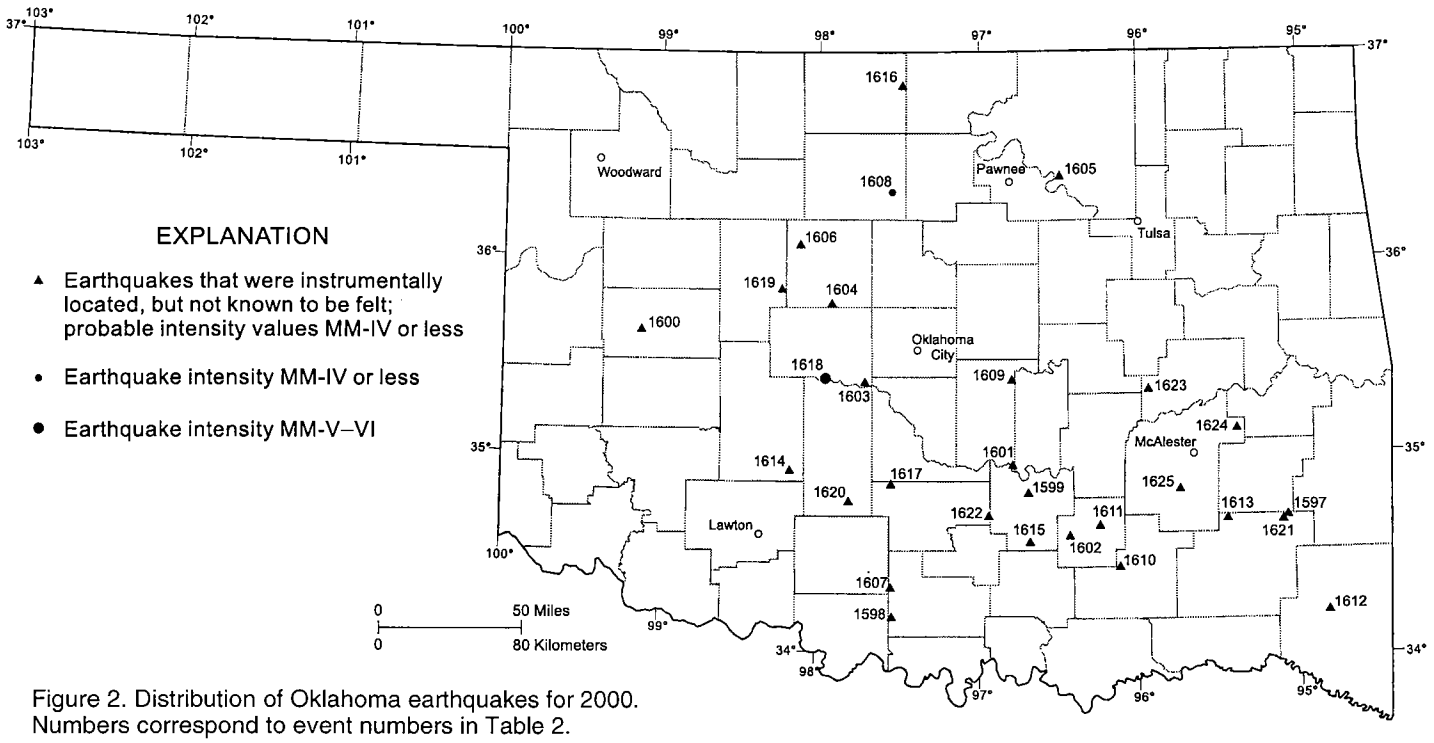

Figure 2. Distribution of Oklahoma earthquakes for 2000. Numbers correspond to event numbers in Table 2.

Each hypocenter is usually run in a preliminary form using the first four or so P and/or S arrivals from about four stations. Later, after all seismograms have been read, a final location is determined. The solutions are added manually to a catalog on the Observatory Web site at http://www.okgeosurvey1.gov/level2/okeqcat/okeqcat.2000.html.

DISTRIBUTION OF OKLAHOMA EARTHQUAKES, 2000

All Oklahoma earthquakes recorded on seismograms from three or more stations are located. In 2000, 29 Oklahoma earthquakes were located (Fig. 2; Table 2). Two earthquakes were reported felt (Table 3). The felt and observed effects of earthquakes generally are given values according to the Modified Mercalli intensity scale, which assigns a Roman numeral to each of 12 levels described by effects on humans, man-made constructions, or natural features (Table 4).

An earthquake was reported felt in southwest Garfield County near Hayward on April 11, 2000. This magnitude 2.6 (mbLg) earthquake produced MM II effects near the epicenter. In Canadian, Grady, and Oklahoma Counties, nine people submitted felt reports for the October 8 earthquake near Union City in Canadian County. This earthquake was reported felt in El Reno, the Union City area, Minco, and northwestern Oklahoma City. This magnitude 2.5 (mbLg) earthquake produced MM V effects near the epicenter. Felt reports ranged from a "sharp jolt" in Minco to a "loud explosion" then "things rattled" near Union City. No damage was reported from either earthquake. The felt area for the Hayward earthquake probably was restricted to a few tens of square kilometers away from the epicentral location. The Union City earthquake had a much larger felt area—approximately 4,000 square kilometers.

In 2000, earthquake-magnitude values ranged from a low of 0.8 (m3Hz) in McIntosh County to a high of 3.0 (m3Hz) in Pushmataha County. Most of the earthquakes occurred in east-central and southeastern Oklahoma, a change from previous years. Three earthquakes were located in Pushmataha County, and several counties—Canadian, Carter, Coal, Garvin, Kingfisher, McIntosh, Pittsburg, and Pontotoc—experienced two earthquakes.

CATALOG

For both preliminary and final locations, the catalog of Oklahoma earthquakes is in HTML (World Wide Web) format; one HTML page contains all of the earthquakes that occurred in one year (a single page lists earthquakes for multiple years prior to 1977). In order to assure absolute uniformity, the catalog is stored only in HTML format. One copy is on a ONENet server. (ONENet is the network of the Oklahoma Regents for Higher Education.) This server copy, at the World Wide Web address http://www.okgeosurvey1.gov, is used both for public distribution and for in-house reference. A second (backup) copy is on a Sun SPARC20 workstation at the Observatory in Leonard.

Each event in the catalog is sequentially numbered and arranged according to date and origin time. The numbering system is compatible with the system used by Lawson and Luza (1980–1990, 1993–2000), Lawson and others (1991, 1992), and for the *Earthquake Map of Oklahoma* (Lawson and Luza, 1995b). The Oklahoma earthquakes article published annually in *Oklahoma Geology Notes* uses an additional sequential event number not found on the World Wide Web catalog.

The dates and times for the cataloged earthquakes are given in UTC. UTC refers to Coordinated Universal Time, formerly Greenwich Mean Time. The first two digits refer to

TABLE 2. — OKLAHOMA EARTHQUAKE CATALOG FOR 2000

Event no.	Date and origin time (UTC)[a]	County	Intensity MM[b]	Magnitudes m3Hz	mbLg	MDUR	Latitude deg N[c]	Longitude deg W[c]	Depth (km)[c]	
1597	Jan 14 10 39 34.94	Pushmataha		3.0	2.9	2.6	34.6735	95.0949	17.57	C
1598	Jan 15 12 35 39.73	Carter		1.9		1.9	34.1818	97.5560	5.00R	C
1599	Jan 17 10 12 18.24	Pontotoc		1.7	1.4	1.7	34.8021	96.6869	5.88	C
1600	Feb 12 08 01 04.04	Custer		1.7		2.0	35.5941	99.0800	5.00R	C
1601	Mar 02 02 17 33.67	Pottawatomie				1.7	34.9477	96.7957	5.00R	C
1602	Mar 18 04 15 50.29	Coal		1.7	1.5	1.4	34.5783	96.4440	16.62	C
1603	Mar 22 01 46 21.38	Canadian		1.7	1.7	1.5	35.3479	97.7176	11.64	C
1604	Mar 22 02 07 06.95	Kingfisher		1.9	1.9	1.7	35.7408	97.8753	11.76	C
1605	Apr 07 03 19 44.78	Osage		1.3		1.3	36.3750	96.4935	5.00R	C
1606	Apr 08 04 31 51.12	Kingfisher		2.0	1.9	2.1	36.0503	98.1158	5.00R	C
1607	Apr 09 03 08 15.99	Carter				1.8	34.3122	97.5601	17.56	C
1608	Apr 11 10 40 56.35	Garfield	II	2.8	2.6	2.2	36.2703	97.5668	17.79	C
1609	Apr 11 19 47 28.26	Pottawatomie		2.6	2.1	1.9	35.3585	96.7921	5.00R	C
1610	Apr 20 17 08 19.88	Atoka		2.2	2.3	1.9	34.4188	96.1152	5.00R	C
1611	May 18 00 31 33.90	Coal				1.4	34.6296	96.2561	1.56	C
1612	May 19 00 28 58.65	McCurtain				1.6	34.2060	94.8465	5.00R	C
1613	May 23 09 12 22.94	Pushmataha		2.2	2.1	2.0	34.6650	95.4628	5.00R	C
1614	Jun 18 15 54 29.58	Caddo		2.2		2.0	34.9170	98.1862	2.28	C
1615	Aug 11 23 54 52.42	Pontotoc		1.6		1.6	34.5591	96.6451	5.00R	C
1616	Aug 20 03 59 44.31	Grant			1.7	1.4	36.7878	97.4832	5.00R	C
1617	Aug 29 08 41 56.98	Garvin		1.6	1.4	1.6	34.8382	97.5591	5.00R	C
1618	Oct 08 10 16 24.77	Canadian	V	2.4	2.5	2.3	35.3917R	97.9411R	5.00R	C
1619	Nov 10 00 14 31.10	Blaine		2.4	2.3	2.3	35.8248	98.2551	5.00R	C
1620	Nov 11 00 14 32.18	Grady		2.4	2.3	2.0	34.7740	97.8066	10.98	C
1621	Dec 20 02 40 51.53	Pushmataha		1.5		1.9	34.6583	95.1029	5.00R	C
1622	Dec 20 18 48 02.95	Garvin		1.8			34.6814	96.9406	5.00R	C
1623	Dec 25 04 51 47.30	McIntosh		0.8		1.4	35.3001	95.9508	5.00R	C
1624	Dec 27 10 48 55.22	Pittsburg		1.2		1.7	35.1154	95.4030	5.00R	C
1625	Dec 30 10 20 58.77	Pittsburg		1.1		1.3	34.8348	95.7356	5.00R	C

[a]UTC refers to Coordinated Universal Time, formerly Greenwich Mean Time. The first two digits refer to the hour on a 24-hour clock. The next two digits refer to the minute, and the remaining digits are the second. To convert to local Central Standard Time, subtract 6 hours.

[b]Modified Mercalli (MM) earthquake-intensity scale (see Table 4). "F" indicates earthquake was reported felt, intensity unknown, generally ≤IV.

[c]If R is preceded by a number in the latitude and/or longitude column(s), the location was restrained to where the earthquake produced the highest Modified Mercalli intensity value(s). 5.0R indicates that the depth was restrained to 5.0 km from the beginning of the calculation. If R is preceded by a number other than 5.0, the depth was restrained at that depth part way through the location calculations. When R does not appear, the number was an unrestrained depth, re-adjusted at every iteration during the location. C refers to the Chelsea velocity model (Mitchell and Landisman, 1971).

the hour on a 24-hour clock. The next two digits refer to the minute, and the remaining digits are the seconds. To convert to local Central Standard Time, subtract 6 hours.

Earthquake magnitude is a measurement of energy and is based on data from seismograph records. The magnitude of a local earthquake is determined by taking the logarithm (base 10) of the largest ground motion recorded during the arrival of a seismic-wave type and applying a standard correction for distance to the epicenter. An increase of one unit in the magnitude value corresponds to a tenfold increase in the amplitude of the earthquake waves. There are several different scales used to report magnitude. Table 2 has three magnitude scales, which are mbLg (Nuttli), m3Hz (Nuttli), and MDUR (Lawson). Each magnitude scale was established to accommodate specific criteria, such as the distance from the epicenter, as well as the availability of certain seismic data.

For earthquake epicenters located 11–222 km from a seismograph station, Otto Nuttli developed the m3Hz magnitude scale (Zollweg, 1974). This magnitude is derived from the following expression:

$$m3Hz = \log(A/T) - 1.63 + 0.87\log(\Delta),$$

where A is the maximum center-to-peak vertical-ground-motion amplitude sustained for three or more cycles of Lg waves, near 3 Hz in frequency, measured in nanometers; T is the period of the Lg waves measured in seconds; and Δ is the great-circle distance from epicenter to station measured in kilometers.

TABLE 3. — EARTHQUAKES REPORTED FELT IN OKLAHOMA, 2000

Event no.	Date and origin time (UTC)[a]	Nearest city	County	Intensity MM[b]
1608	Apr 11 10 40 56.35	Hayward	Garfield	II
1618	Oct 08 10 16 24.77	Union City	Canadian	F

[a]UTC refers to Coordinated Universal Time, formerly Greenwich Mean Time. The first two digits refer to the hour on a 24-hour clock. The next two digits refer to the minute, and the remaining digits are the second. To convert to local Central Standard Time, subtract 6 hours.

[b]Modified Mercalli (MM) earthquake-intensity scale (see Table 4). "F" indicates earthquake was reported felt, intensity unknown, generally ≤IV.

TABLE 4. — MODIFIED MERCALLI (MM) EARTHQUAKE-INTENSITY SCALE (Abridged) (Modified from Wood and Neumann, 1931)

I	Not felt except by a very few under especially favorable circumstances.
II	Felt only by a few persons at rest, especially on upper floors of buildings. Suspended objects may swing.
III	Felt quite noticeably indoors, especially on upper floors of buildings. Automobiles may rock slightly.
IV	During the day felt indoors by many, outdoors by few. At night some awakened. Dishes, doors, windows disturbed. Automobiles rocked noticeably.
V	Felt by nearly everyone, many awakened. Some dishes, windows, etc., broken; unstable objects overturned. Pendulum clocks may stop.
VI	Felt by all; many frightened and run outdoors.
VII	Everybody runs outdoors. Damage negligible in buildings of good design and construction. Shock noticed by persons driving automobiles.
VIII	Damage slight in specially designed structures; considerable in ordinary substantial buildings; great in poorly built structures. Fall of chimneys, stacks, columns. Persons driving automobiles disturbed.
IX	Damage considerable even in specially designed structures; well-designed frame structures thrown out of plumb. Buildings shifted off foundations. Ground cracked conspicuously.
X	Some well-built wooden structures destroyed; ground badly cracked, rails bent. Landslides and shifting of sand and mud.
XI	Few if any (masonry) structures remain standing. Broad fissures in ground.
XII	Damage total. Waves seen on ground surfaces.

In 1979, St. Louis University (Stauder and others, 1979) modified the formulas for m3Hz. This modification was used by the OGS Observatory beginning January 1, 1982. The modified formulas had the advantage of extending the distance range for measurement of m3Hz out to 400 km, but also had the disadvantage of increasing m3Hz by about 0.12 units compared to the previous formula. Their formulas were given in terms of log(A) but were restricted to wave periods of 0.2–0.5 sec. In order to use log(A/T), we assumed a period of 0.35 sec in converting the formulas for our use. The resulting equations are:

(epicenter 10–100 km from a seismograph)

$$m3Hz = \log(A/T) - 1.46 + 0.88 \log(\Delta)$$

(epicenter 100–200 km from a seismograph)

$$m3Hz = \log(A/T) - 1.82 + 1.06 \log(\Delta)$$

(epicenter 200–400 km from a seismograph)

$$m3Hz = \log(A/T) - 2.35 + 1.29 \log(\Delta).$$

Otto Nuttli's (1973) earthquake magnitude, mbLg, for seismograph stations located between 55.6 and 445 km from the epicenter, is derived from the following equation:

$$mbLg = \log(A/T) - 1.09 + 0.90 \log(\Delta).$$

Where seismograph stations are located between 445 and 3,360 km from the epicenter, mbLg is defined as:

$$mbLg = \log(A/T) - 3.10 + 1.66 \log(\Delta),$$

where A is the maximum center-to-peak vertical-ground-motion amplitude sustained for three or more cycles of Lg waves, near 1 Hz in frequency, measured in nanometers; T is the period of Lg waves measured in seconds; and Δ is the great-circle distance from epicenter to station measured in kilometers.

The MDUR magnitude scale was developed by Lawson (1978) for earthquakes in Oklahoma and adjacent areas. It is defined as:

$$MDUR = 1.86 \log(DUR) - 1.49,$$

where DUR is the duration or difference, in seconds, between the Pg-wave arrival time and the time the final coda amplitude decreases to twice the background-noise amplitude. Before 1981, if the Pn wave was the first arrival, the interval between the earthquake-origin time and the decrease of the coda to twice the background-noise amplitude was measured instead. Beginning January 1, 1982, the interval from the beginning of the P wave (whether it was Pg, P*, or Pn) to the decrease of the coda to twice the background-noise amplitude was used.

Earthquake detection and location accuracy have been greatly improved since the installation of the statewide network of seismograph stations. The frequency of earthquake events and the possible correlation of earthquakes to specific tectonic elements in Oklahoma are being studied. It is hoped that this information will provide a more complete data base that can be used to develop numerical estimates of earthquake risk, giving the approximate frequency of the earthquakes of any given size for various regions of Oklahoma. Numerical risk estimates could be used for better design of large-scale structures, such as dams, high-rise buildings, and power plants, as well as to provide the necessary information to evaluate insurance rates.

ACKNOWLEDGMENTS

Todd McCormick, James King, and Amie Friend maintain the OGS Observatory at Leonard. Volunteer seismograph-station operators and landowners at various locations in Oklahoma make possible the operation of a statewide seismic network.

This work was funded directly by the Oklahoma Geological Survey. The GSE digital seismic system, provided by the Defense Advanced Research Projects Agency/Nuclear Monitoring Research Office, considerably enhanced the OGS's ability to analyze Oklahoma earthquakes. A borehole seismic system, a joint project with the Lawrence Livermore National Laboratories, was useful in recording Oklahoma earthquakes. The three-component broadband Guralp seismometer in the 864-m borehole and the Guralp data acquisition system were funded by a DARPA-DEPSCoR grant. The Observatory exists because of building and land-purchase gifts from Jersey Production Research Co. (now merged into Exxon) and the Sarkeys Foundation.

REFERENCES CITED

Docekal, Jerry, 1970, Earthquakes of the stable interior, with emphasis on the Midcontinent: University of Nebraska, Lincoln, unpublished Ph.D. dissertation, v. 1, 169 p.; v. 2, 332 p.

Indian Pioneer Papers [date unknown], Interview, Eliza Ross: Western History Collections, University of Oklahoma Libraries, Norman, v. 78, p. 164–167.

Kalb, Bill, 1964, Earthquakes that shook Oklahoma: Orbit Magazine—The Sunday Oklahoman, Oklahoma City, September 27, p. 4–7.

Lawson, J. E., Jr., 1978, A preliminary duration magnitude scale for local and regional earthquakes recorded at Oklahoma seismograph stations: Oklahoma Geological Survey Observatory Open-File Report, 14 p.

——— 1980, Geophysical observatory establishes continuous time synchronization: Oklahoma Geology Notes, v. 40, p. 214.

Lawson, J. E., Jr.; and Luza, K. V., 1980, Oklahoma earthquakes, 1979: Oklahoma Geology Notes, v. 40, p. 95–105.

——— 1981, Oklahoma earthquakes, 1980: Oklahoma Geology Notes, v. 41, p. 140–149.

——— 1982, Oklahoma earthquakes, 1981: Oklahoma Geology Notes, v. 42, p. 126–137.

——— 1983, Oklahoma earthquakes, 1982: Oklahoma Geology Notes, v. 43, p. 24–35.

——— 1984, Oklahoma earthquakes, 1983: Oklahoma Geology Notes, v. 44, p. 32–42.

——— 1985, Oklahoma earthquakes, 1984: Oklahoma Geology Notes, v. 45, p. 52–61.

——— 1986, Oklahoma earthquakes, 1985: Oklahoma Geology Notes, v. 46, p. 44–52.

——— 1987, Oklahoma earthquakes, 1986: Oklahoma Geology Notes, v. 47, p. 65–72.

——— 1988, Oklahoma earthquakes, 1987: Oklahoma Geology Notes, v. 48, p. 54–63.

——— 1989, Oklahoma earthquakes, 1988: Oklahoma Geology Notes, v. 49, p. 40–48.

——— 1990, Oklahoma earthquakes, 1989: Oklahoma Geology Notes, v. 50, p. 68–76.

——— 1993, Oklahoma earthquakes, 1992: Oklahoma Geology Notes, v. 53, p. 51–62.

——— 1994, Oklahoma earthquakes, 1993: Oklahoma Geology Notes, v. 54, p. 57–68.

——— 1995a, Oklahoma earthquakes, 1994: Oklahoma Geology Notes, v. 55, p. 51–63.

——— 1995b, Earthquake map of Oklahoma (earthquakes shown through 1993): Oklahoma Geological Survey Map GM-35, scale 1:500,000.

——— 1996, Oklahoma earthquakes, 1995: Oklahoma Geology Notes, v. 56, p. 49–63.

——— 1997, Oklahoma earthquakes, 1996: Oklahoma Geology Notes, v. 57, p. 40–52.

——— 1998, Oklahoma earthquakes, 1997: Oklahoma Geology Notes, v. 58, p. 60–72.

——— 1999, Oklahoma earthquakes, 1998: Oklahoma Geology Notes, v. 59, p. 64–77.

——— 2000, Oklahoma earthquakes, 1999: Oklahoma Geology Notes, v. 60, p. 33–39.

Lawson, J. E., Jr.; Luza, K. V.; and Moss, Dan, 1991, Oklahoma earthquakes, 1990: Oklahoma Geology Notes, v. 51, p. 50–61.

Lawson, J. E., Jr.; Luza, K. V.; Brown, R. L.; and Moss, Dan, 1992, Oklahoma earthquakes, 1991: Oklahoma Geology Notes, v. 52, p. 48–59.

Luza, K. V., 1978, Regional seismic and geologic evaluations of Nemaha uplift, Oklahoma, Kansas, and Nebraska: Oklahoma Geology Notes, v. 38, p. 49–58.

Mitchell, B. J.; and Landisman, M., 1971, Geophysical measurements in the Southern Great Plains, the structure and physical properties of the Earth's crust: American Geophysical Union Geophysical Monograph 14, p. 77–93.

Mykkeltveit, Svein; Ringdal, Frode; Kvaerna, Tormad; and Alewine, R. W., 1990, Application of regional arrays in seismic verification: Seismological Society of America Bulletin, v. 80, p. 1777–1801.

Nuttli, O. W., 1973, Seismic wave attenuation and magnitude relations for eastern North America: Journal of Geophysical Research, v. 78, p. 876–885.

Ross, D. H. (ed.), 1882, Shake: Cherokee Advocate, Friday, October 27, p. 1.

Schweitzer, Johannes, 1997, HYPOSAT—a new routine to locate seismic events: NORSAR Science Reports, 1-97/98, November 1997, p. 94–102.

Stauder, W.; Hermann, R.; Singh, S.; Reidy, D.; Perry, R.; and Morrissey, Sean-Thomas, 1979, Central Mississippi Valley Earthquake Bulletin: First Quarter 1979, no. 19, 50 p.

Stover, C. W.; Reagor, B. G.; Algermissen, S. T.; and Lawson, J. E., Jr., 1981, Seismicity map of the State of Oklahoma: U.S. Geological Survey Miscellaneous Field Studies Map MF-1352, scale 1:1,000,000.

Tarbuck, E. J.; and Lutgens, F. K., 1990, The earth—an introduction to physical geology: Merrill Publishing Co., Columbus, Ohio, 651 p.

von Hake, C. A., 1976, Earthquake history of Oklahoma: Earthquake Information Bulletin, v. 8, p. 28–30.

Wells, L. L., 1975, Young Cushing in Oklahoma Territory: Frontier Printers, Stillwater, Oklahoma, 221 p.

Wood, H. O.; and Neumann, Frank, 1931, Modified Mercalli intensity scale of 1931: Seismological Society of America Bulletin, v. 21, p. 227–283.

Zollweg, James, 1974, A preliminary study of the seismicity of the central United States, 1974: St. Louis University unpublished undergraduate report, 15 p.

OCGS Geological Library and Office Moved

The Geological Library and Office of the Oklahoma City Geological Society (OCGS) has moved to larger and more convenient space on the 9th Floor of the Center Building in the First National Center, Oklahoma City. The library is used by more than 700 members who are active in the exploration for and development of oil and gas resources in Oklahoma and neighboring states.

The library maintains well drilling records, electric and lithologic well logs, and oil and gas production data from Oklahoma as well as adjoining states. The members have access to a wide range of databases and programs dealing with mapping, data handling, and oil and gas production at computer work stations available in the library.

Since its beginning in 1966, the Geological Library has grown into one of the premier repositories of data and references pertaining to petroleum geology and the petroleum industry in the southwestern United States.

This year, the OCGS also celebrates the 80th anniversary of its founding in Oklahoma City in 1921. The OCGS affiliated with the American Association of Petroleum Geologists in 1931 and is one of its earliest member societies. The society was incorporated in the State of Oklahoma as a nonprofit corporation in 1966, and now has more than 1,000 members primarily composed of geologists and individuals connected to the petroleum industry. During its 80-year history, the group has held meetings featuring subjects pertaining to petroleum geology, conducted geological field trips, granted scholarships to university geology students, and given monetary awards to State Science Fair participants. The OCGS also publishes reports on oil and gas fields in Oklahoma and other geological subjects, and provides transactions of geological meetings it has sponsored.

In 1951, the Society began publishing its periodical the *Shale Shaker*, the journal of the Oklahoma City Geological Society. The *Shale Shaker* is devoted to the purposes of keeping the membership informed of activities of the Society and printing technical articles and news items related to the geological profession.

The OCGS now can be reached at:
120 N. Robinson, Suite 900 Center,
Oklahoma City, OK 73102
Phone:(405) 236-8086
Fax: (405) 236-8085
Web site: www.ocgs.org

Arbuckle Aquifer Water Table Dropping

The water table in the Arbuckle aquifer in south-central Oklahoma is at its lowest level since October 1984, the U.S. Geological Survey has announced. The water table is now more than 118 feet below land surface in an observation well near Fittstown, about 48 feet lower than it was in May 1990. This well has been monitored by the USGS since 1958.

Normally the water table in the Arbuckle aquifer rises and falls about 20 feet each year at this well, usually reaching a low point in the late fall, then rising with winter and spring rains. The annual low point has been dropping every year since the early 1990s. Average monthly rainfall in south-central Oklahoma also has been declining during the same period. Rainfall is the source of water in the Arbuckle aquifer.

The water table drops when more water is leaving the aquifer than is recharging it. Water leaves the aquifer by natural discharge to springs and streams, vegetation that has roots below the water table, and pumpage. Rainfall infiltrates through soil and recharges the aquifer, mostly during the winter when vegetation is dormant. Long periods without rain mean that there will be more water leaving the aquifer than recharging it. The water table is still higher than it was in May 1967 when it was 128 feet below land surface.

The lower water table in this well directly reflects the regional rainfall. Continuous monitoring of ground-water levels in wells is a good approach to tell if an area is still in a hydrologic drought. Fall rainfall may relieve meteorological and agricultural droughts and streamflow may rise for a short time, but if there isn't enough rain over several months to recharge the aquifer, the water table will continue to drop and streamflow will be very low again next summer. Some streams will be dry.

The Arbuckle aquifer discharges to springs and streams in south-central Oklahoma, including the Chickasaw National Recreation Area. It also discharges to flowing wells near Sulphur. As the water table drops, there is less discharge to these springs, streams, and wells. They will dry up eventually if the water table continues to drop. Byrds Mill Spring, near Fittstown, is fed by water discharging from the Arbuckle and flow in the spring varies as the water table varies. Byrds Mill Spring is the water supply for the City of Ada. The Blue River drains the aquifer as well and low flow is discharge from the Arbuckle aquifer. Flow in the Blue River also rises and falls as the water table rises and falls.

About 3.75 million gallons per day of water from the Arbuckle and associated Simpson aquifers were used in 1995, mostly for water supply but also for livestock, irrigation, and industrial supplies.

The U.S. Geological Survey water-table data for this well are available at: ok.water.usgs.gov/public/gwsites/fitts. html. For more information, contact Kathy Peter, U.S. Geological Survey, Water Resources Division, 202 N.W. 66th St., Bldg. 7, Oklahoma City, OK 73116; phone: (405) 810-4417; email: kdpeter@usgs.gov.

new OGS publications

CIRCULAR 104

- *edited by* Kenneth S. Johnson
- 233 pages
- Paperbound, laminated cover
- $15

Pennsylvanian and Permian Geology and Petroleum in the Southern Midcontinent, 1998 Symposium

Contained in this volume are papers dealing with the search for, and production of, oil and gas resources from reservoirs of Pennsylvanian and Permian age in the southern Midcontinent. The research focuses on the reservoirs, geologic events, and petroleum of rocks deposited during the Pennsylvanian and Permian Periods. Clastic and carbonate reservoirs of this age are major sources of oil and gas in the southern Midcontinent, and they have great potential for additional recovery using advanced technologies.

The 30 papers and abstracts in this book concentrate on geology, depositional settings, diagenetic history, reservoir characterization, sequence stratigraphy, exploration, petroleum production, coalbed methane, and enhanced oil recovery. The research originally was presented at a two-day workshop held in April 1998 in Norman, Oklahoma, cosponsored by the OGS and the National Petroleum Technology Office of the U.S. Department of Energy. The meeting drew more than 200 representatives from industry, government, and academia. In describing these petroleum reservoirs of Pennsylvanian and Permian age, the researchers involved in this meeting increased our understanding of how the geologic history of an area can affect reservoir heterogeneity and the ability to efficiently recover hydrocarbons.

Among the reservoirs discussed are: Springer, Morrow, Red Fork, "Granite Wash," Red Cave, Clear Fork, and other Pennsylvanian and Permian units. Study areas include many major fields in Oklahoma, as well as sites in Kansas, Colorado, Texas, and New Mexico. As oil prices have increased recently, a greater interest in drilling in the State makes these papers a valuable resource for explorationists and operators in Oklahoma.

GUIDEBOOK 33

- *by* Thomas M. Stanley
- 73 pages
- Paperbound, laminated cover
- $8

Stratigraphy and Facies Relationships of the Hunton Group, Northern Arbuckle Mountains and Lawrence Uplift, Oklahoma

Part of a continuing series that provides information and technical assistance to Oklahoma's oil and gas operators, this guidebook presents information on the basics of Hunton Group stratigraphy and lithofacies analysis as they are exemplified at the surface in the Arbuckle Mountains. An attempt to bridge the gap between subsurface mapping and log correlations with these surface outcrops also is made. The guidebook is divided into two parts: Part I, general stratigraphy and lithofacies of the Hunton Group as they are expressed throughout the Arbuckle region; and Part II, descriptions of the nine field-trip stops of the northern outcrop belt and Lawrence uplift. The guidebook is a companion to OGS Special Publication 2000-2, *Hunton Play in Oklahoma (Including Northeast Texas Panhandle)*, by Kurt Rottmann and others, which contains the information covered in a workshop on the Hunton Group play.

The guidebook was prepared for a field trip conducted by the OGS in May 2001 to show all aspects of Hunton facies, but particularly those that form good hydrocarbon reservoirs in the subsurface. Surface gamma-ray profiles of the outcrops are compared to subsurface log signatures. Interpretations of carbonate depositional environments are emphasized in both parts of this guidebook, with the understanding that a correct interpretation of facies and depositional environment is essential for predicting potential hydrocarbon reservoirs. Guidebook author Thomas M. Stanley led the field trip.

Circular 104 and **Guidebook 33** can be purchased by mail from the Survey at 100 E. Boyd, Room N-131, Norman, OK 73019; fax 405-325-7069. To mail order, add 20% to the cost for postage, with a minimum of $2 per order.

All OGS publications can be purchased over the counter at the OGS Publication Sales Office, 1218-B W. Rock Creek Road, Norman; phone (405) 360-2886, fax 405-366-2882, e-mail ogssales@ou.edu. Request the OGS *List of Available Publications* for current listings and prices.

Upcoming meetings

SEPTEMBER 2001

Society of Exploration Geophysicists, International Exposition and Annual Meeting, September 9–14, 2001, San Antonio, Texas. Information: SEG Business Office; (918) 497-5500; fax 918-497-5557; website—http://seg.org.

The Society for Organic Petrology, Annual Meeting, September 23–26, 2001, Houston, Texas. Information: Cole Robison, Texaco Group, Inc., E&P Technology Division, 3901 Briarpark Dr., Houston, TX 77042; (713) 432-6828; fax 713-838-4628; e-mail: robiscr@texaco.com; website—http://www.tsop.org/mtghst.htm.

Society of Petroleum Engineers, Annual Meeting, September 30–October 3, 2001, New Orleans, Louisiana. Information: website—http://www.spe.org/.

OCTOBER 2001

Association of Engineering Geologists/American Institute of Professional Geologists, Joint Meeting, October 3–6, 2001, St. Louis, Missouri. Information: Larry Rosen, AEG co-chair, (314) 392-0050; or John Howard, AIPG co-chair, (314) 209-3609; website—http://www.aipg.org/.

Gulf Coast Association of Geological Societies, Annual Convention, October 17–19, 2001, Shreveport, Louisiana. Information: Thomas C. Wyche, C.H.C. Gerard and Associates, 625 Market St., Suite 250, Shreveport, LA 71101; (318) 221-0761; fax 318-221-8835; e-mail: tcwych@aol.com.

DECEMBER 2001

Interstate Oil and Gas Compact Commission, Annual Meeting, December 9–11, 2001, Santa Fe, New Mexico. Information: IOGCC, P.O. Box 53127, Oklahoma City, OK 73152; (405) 525-3556; fax 405-525-3592; e-mail: iogcc@iogcc.state.ok.us; website—http://www.iogcc.state.ok.us.

MARCH 2002

National Earth Science Teachers Association, Annual Meeting, March 27–30, 2002, San Diego, California. In-formation: NESTA, 2000 Florida Ave., N.W., Washington, DC 20009; (202) 462-6910; fax 202-328-0566; e-mail: fireton@kosmos.agu.org.

American Association of Petroleum Geologists, Annual Convention and Exhibition, March 10–13, 2002, Houston, Texas. Information: AAPG, 1444 S. Boulder Ave., P.O. Box 979, Tulsa, OK 74101; (800) 364-2274 or (918) 560-2679; fax 800-281-2283 or 918-560-2684; website—http://www.aapg.org/.

Oklahoma Coalbed-Methane Workshop and Field Trip

October 10–11, 2001 • Poteau, Oklahoma

The Oklahoma Geological Survey will host the fifth Oklahoma Coalbed-Methane Workshop and Field Trip on October 10–11. The technical presentations will be at Carl Albert State College in Poteau, Oklahoma, on Wednesday, October 10. Some six to eight speakers will present an overview of coal as a gas source rock and reservoir, and examine factors affecting coalbed-methane (CBM) producibility, Oklahoma coal geology, Oklahoma CBM activity, and Oklahoma CBM economic potential and completion practices. A workshop manual will be included with the registration.

An optional field trip will visit active coal mines, coal outcrops, and a CBM field operation in the southeast Oklahoma portion of the Arkoma basin on Thursday, October 11, following the technical sessions. Enrollment for the field trip is limited, so register early. For further information, contact Michelle Summers at the Oklahoma Geological Survey, phone (405) 325-3031 *or* (800) 330-3996; fax 405-325-7069; e-mail: ogs@ou.edu; website—http://www.ou. edu/special/ogs-pttc/.

Information available for Earth Science Week 2001

Across the nation, the week of October 7–13 will be celebrated as Earth Science Week 2001.

In recognition of Earth Science Week in Oklahoma, the Oklahoma Geological Survey is preparing a publication titled *Oklahoma's Energy Landscape,* which will describe Oklahoma's energy consumption, imports, and exports regarding oil, gas, coal, and the generation of electricity. For information, contact Dan Boyd, (405) 325-3031, e-mail: dtboyd@ou.edu. OGS publications released for past Earth Science Week celebrations also are still available.

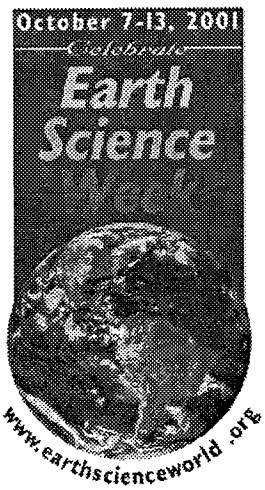

The American Geological Institute, the sponsor organization for Earth Science Week, offers free kits (one per individual) and information to help teachers, field-trip leaders, and others prepare for Earth Science Week. Contact: Earth Science Week, American Geological Institute, 4220 King St., Alexandria, VA 22302; phone (703) 379-2480; fax 703-379-7563; website—http://www.earthscienceworld.org/.

AAPG Mid-Continent Section Meeting
September 30–October 2, 2001 ✪ Amarillo, Texas

The Panhandle Geological Society and the Mid-Continent Section of the American Association of Petroleum Geologists are co-hosting the 2001 AAPG Mid-Continent Section meeting. The theme is "Exploitation—Exploration: 21st Century Technology."

Technical Program

Monday, October 1

Magneto-Stratigraphic Correlation and Dating of West Texas and New Mexico Later Permian Strata

The Elm Creek Formation (Wichita-Albany Group) in North-Central Texas

Coalbed-Methane Potential and Exploration Strategies for the Mid-Continent Region

Considerations for Coalbed Methane in Kansas, Based on the Kansas Coal Resource

Surface to Subsurface Correlation of Methane-Producing Coals, Northeast Oklahoma Shelf Area

An Update of Oklahoma Coalbed-Methane Activity

Cleats in Coal of Eastern Oklahoma

Reserve Estimates for Naturally Fractured Reservoirs

New Data on the Palo Pinto Formation (Missourian, Pennsylvanian), Northeastern Palo Pinto County, Texas

All Faults Are Not Created Equal

Tuesday, October 2

Could Groundwater Trading be the "Oil Patch" of the 21st Century?

Natural Gas, Uranium, Helium, Radon, Arsenic, and Groundwater Quality of the Ogallala Aquifer

Graphic Results—Panhandle Area Ogallala Groundwater Model—1950–2050

Permian Basin Petroleum Systems Investigations: Inferences from Oil Geochemistry and Source Rocks

SP Revisited

Resistivity Logs Revisited

Deltaic Progradation During Maximum Marine Transgression, the Heebner Shale Member of the Oread Limestone

Population and Energy, 2001–2100

Characteristics of Accommodation Space Changes of Mesozoic in Songlia Basin, East China

The Deposition and Diagenesis of the Caddo Algal Mounds, Caddo Limestone (Pennsylvanian), Stephens County, Texas

Compartmentalization of Overpressured Reservoirs in the Anadarko Basin

Amarillo, Texas—Home of World Class Production and World Class Geology

How Seismic Ray Trace Modeling Can Enhance the Interpretation of Seismic Data from Complex Subsurface Structures: An Example from the Wichita Mountains Frontal Zone, Southern Oklahoma

Stratigraphic Adventures in the Granite Wash of Hartley County: A Case History

Horizontal Drilling in the Texas Panhandle

Poster Sesssions

NMR Relaxation Times and Related Pore Geometry in the Morrow Group (Pennsylvanian), Hemphill County

The Petrology and Tectonics of the Precambrian Panhandle Terrain in West Texas

Suitability of the Wolfcamp Series as a High-Volume Disposal Zone in the Palo Duro Basin

Upper Mississippian (Chester) Ooid Shoals: Austin Upper Mississippian Field, New Mexico, and Mocane Laverne Field, Oklahoma, and their Relation to North American Chester Paleogeography

Sequence Stratigraphic Control on Reservoir Quality in Morrow Sandstone Reservoirs, Northwestern Shelf, Anadarko Basin

Characteristics of Turbidity Flow Sedimentation and Effects on Reservoir Property in Early Tertiary of Dongying Sag, Bohaiwan Basin, East China

Short Course

Methods in Exploitation/Exploration: Computer Mapping

Field Trips

Palo Duro Canyon, *Sept. 30*

Nichols-Harrington Power Plant Stations, *Oct. 1*

✪

Further information: Bill Knebusch, General Chairman, 1616 S. Kentucky, Suite 260D, Amarillo, TX 79102; phone (806) 352-7520; e-mail: billybob@arn.net.

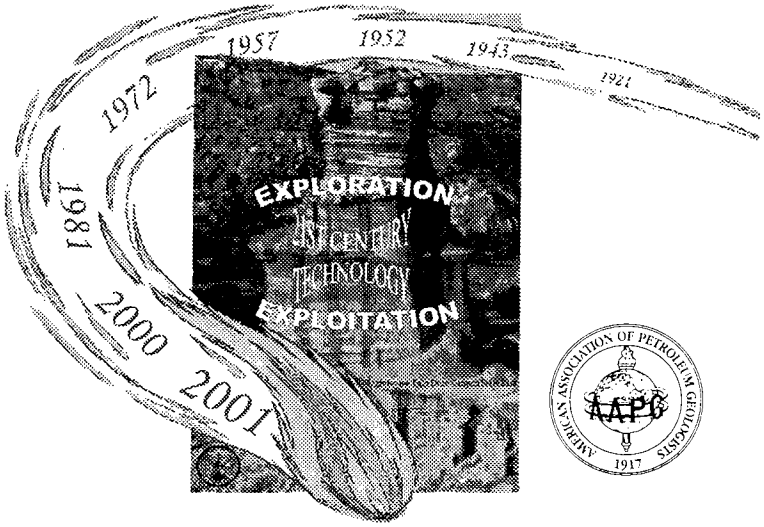

GSA Annual Meeting and Exposition

November 1–10, 2001 ~ Boston, Massachusetts

A Geo-Odyssey

The Geological Society of America invites you to participate in its Annual Meeting in Boston this November. And what a meeting it will be! Superb science, great facilities, exciting field trips and workshops, and wonderful food and entertainment—all in a modern, vibrant city that retains an old-world flair.

This meeting has something for everyone. Note the breadth and quality of the proposed Pardee Symposia and Topical Sessions. These reflect the cutting edge and diversity of our science at the beginning of the third millennium. In addition, eight Hot Topic forums will cover current or controversial issues and dozens of discipline sessions.

All the technical sessions will be held in the modern and recently renovated facilities of the Hynes Convention Center in the heart of downtown Boston. Add in the numerous division and society meetings, alumni reunions, and the opportunity to meet and network with old friends and new, and you have a meeting you can't afford to miss.

More than 25 diverse field trips, with excursions that will appeal to every specialty, are planned. From the mountains of New England to the beaches of Maine and even to subterranean Boston, there is an excursion just for you. The meeting also includes short courses, workshops, and special forums.

And, there's Boston itself! Space doesn't even begin to allow room for a list of the things to do and see in this charming and modern, yet very historical, city. Museums, shopping, fine dining, Irish pubs—you name it, Boston has it. The action this November will be at GSA Boston. So come, participate, and enjoy!

~ *J. Christopher Hepburn*
Chairman

GSA Annual Meeting Agenda

PARDEE KEYNOTE SYMPOSIA ~

Geobiology: Applications to Sedimentary Geology

Melt in the Crust and Upper Mantle: How Much, Where, for How Long, and What Significance for Geodynamics?

Nanogeology: The Application of Nanotechnology in Earth Sciences

Ophiolites as Problem and Solution in the Evolution of Geological Thinking

The Emerging Discipline of Medical Geology

The Future of Biogeochemistry: A Symposium in Honor of Harold C. Helgeson

The Watershed Within: Scientific and Moral Reflections on Water in the 21st Century

Water's Many Forms in the Solar System: Implications for Geology, Exploration, and Life

TOPICAL SESSIONS ~

Arc Terranes in the Appalachians and Caledonides and Their Role in Paleozoic Orogenesis

Proterozoic Tectonic Evolution of the Grenville Orogen in Eastern North America

Focus on IGCP: Modern and Ancient Plate Boundaries and Orogens

Crustal Architecture of Rifted Continental Margins

Melt in the Crust and Upper Mantle: How Much, Where, for How Long, and What Significance for Geodynamics?

Evolution of the Precambrian Earth

The Proterozoic of the Eastern Midcontinent and Beyond

"Traces" of Soil Ecosystems through the Phanerozoic: New Insights into Terrestrial Paleoecology, Paleohydrology, and Paleoclimate

New Insights into Late Ordovician Climate, Oceanography, and Tectonics

Holocene Climate Change: Seasonal Variability to Centennial Trends

Sulfur Cycling in Precambrian to Recent Ocean-Atmosphere Systems: A Session Honoring the Career of William T. Holser

Stratigraphic Paleobiology

Foraminifera: Barometers of the Biotic and Abiotic World

Partnerships in Paleontology: Involving the Public in Collaborative Research

Special Session in Honor of Half Zantop

Insects and Terrestrial Arthropods in the Fossil Record: Are So Many Really Represented by So Few?

The Fossil Record of Fire: Recognition and Effects

Radiometric Dating in a Sequence Stratigraphic Framework, Paleozoic through Cenozoic

New Perspectives on the Character and Origin of Late Cretaceous–Cenozoic Sequences on the U.S. Atlantic Margin

Near-Surface Stratigraphic Heterogeneity Beneath the Coastal Plain and Continental Shelf of Eastern North America: Spatial and Temporal Influences on Framework Geology, Processes, Sedimentation, and Morphology

Recent Advances in Deep-Water Facies Models

Quaternary Stratigraphy in Glaciated Terranes: Techniques, Tools, and Mapping

Sediment-Hosted Lead-Zinc Deposits: Roles of Basin Evolution, Tectonics, and Geochemistry in Ore Genesis

Dynamics of Sediments and Sedimentary Environments: A Session in Honor of John B. Southard

Geochemistry of Siliciclastic Materials: Provenance, Paleoclimates, and Plate Tectonic Settings

Geochemistry of Organic-Rich Sediments from Estuaries, Continental Shelves, Basins, and Upwelling Zones

Evaporite Systems: The Geology, Paleontology, and Biology of Evaporite and Near-Evaporite Systems in Both Terrestrial and Extraterrestrial Environments

Anoxia and Black Shale Deposition

High-Resolution Investigations of the Morphodynamics and Sedimentary Evolution of Estuaries

Linking Sediment Dynamics and Stratigraphy in Modern-Holocene Estuaries

The Margins of Reefs and Carbonate Platforms

America's Coastal Crisis—Providing the Geoscience Information/Communication Needed to Conserve and Protect Coastal Resources

Coastal Erosion Programs: Collaborative Geologic Research in Action

Coastal Geology of the National Parks

Diffusive Transport Processes in the Subsurface

Uncertainty in Vadose Zone Flow and Transport Prediction

Recent Advancements in Aquifer Hydraulics and Their Applications to Aquifer and Vadose Zone Characterization, Remediation, and Dewatering

Flow and Transport in Fractured Aquifers—From Field Characterization to Model Construction

Geochemistry of Karst Waters: A Window on Hydrogeology and Biota

Isotopic Tracers and Thermal Anomaly Data as Constraints on Groundwater Flow Patterns and Climate History within Sedimentary Systems

Groundwater Availability Modeling

Groundwater Discharge to Estuaries

Iron in Sedimentary Aquifers: Biological, Chemical, and Physical Controls on Iron Mobility

Hydrology and Hydrogeology of Extreme Environments

Borehole Geophysical Analysis Techniques for the Definition of Aquifer Properties

Applications of Sedimentology and Geophysics in Hydrogeology

Developing Countries Session: Sustainable Groundwater Management in Developing Countries for Protecting the Quality and Quantity of Groundwater

Application of Geochemistry to Understanding Groundwater–Surface Water Interactions

Novel Approaches to Tracing Groundwater Flow Systems and Aquifer Processes: Applications of Isotopic and Trace Element Data

High-Resolution Geochemical Bioarchives: Recognition of Signals and Implications for Evolution, Paleoecology, and Paleoclimatology

Novel Applications of Bulk and Compound Specific Stable and Radiogenic Isotopes for the Solution of Problems in Organic Geochemistry

Geologic Research and Projects for Understanding 21st Century Engineering Geology

Geology and Tunneling: Case Histories

Case Histories in Site Characterization

The Geologic and Human Landscape of Prehistoric Mines and Quarries

Geology Applied to Gas Works Site Characterization

Evaluation of Sources, Aggregates, Quarries, Construction Materials, and Engineering Structures Using Field and Laboratory Techniques

Construction and Geology of the Massachusetts Water Resources Authority Tunnel, Eastern Massachusetts

Rheological Effects of Fluid-Rock Interactions at Depth: From Experimental Constraints to Interpretations of Field Observations

Rock Slope Stability in Surface and Underground Excavations

Natural Arsenic in Groundwater: Science, Regulation, and Health Implications

Munitions: Sources, Fate, and Transport

Contributions of High-Resolution Geophysics to Understanding Neotectonics and Seismic Hazard

Nothing Ventured, Nothing Gained: Geology and Risk Assessment in the 21st Century

Erosion of Non-Lithified Sediments: Observations and Models from Millimeter to Hillslope Scales

Coal Systems Analysis: A New Approach to the Understanding of Coal Formation, Coal Quality and Environmental Considerations, and Coal as a Source Rock for Hydrocarbons

Archaeological Geology and the Pleistocene-Holocene Transition

Old World Archaeology and Quaternary Environments

Geobiography: Life Histories of Geologists as a Way to Understand How Science Operates

Ophiolites as Problem and Solution in the Evolution of Geological Thinking

Prospecting for Humor in a Geological Vein: Mining a Renewable Resource

Geoscience Information: A Dynamic Odyssey

Databases to Knowledge Bases: The Informatics Revolution

Geoinformatics: Extracting Knowledge from the Rock Record Through Construction of Disciplinary Databases and Information Networks

Applications and New Opportunities in Geologic Remote Sensing

Geology in the National Parks: Research, Mapping, Education, and Interpretation

Increasing Student Engagement in Geoscience Courses Through Information Technology: A Component of Enrollment Management

Academic Training of Engineering Geologists from a Practitioner's Perspective

Innovative Approaches to Undergraduate Teaching of Oceanography

Models and Approaches to Teaching Geology to Pre- and In-Service Teachers

Strategies for Promoting Active Learning in Large Entry-Level Courses

Models of Successful Undergraduate Research Programs in the Geosciences

Sigma Gamma Epsilon Student Research Poster Session

Recreating Undergraduate Majors and Curriculum—Approaches for a New Century

The Coming Revolution in Earth and Space Science Education

What Can I Do with a Major in the Geosciences? Advising Students in Future Career Decisions

Fossil Fuel on Federal Land

New Topics in Grenville Tectonics: A New Look at Some Old Rocks

Iron-Oxide(-Copper-Gold) Systems—Deposit Studies to Global Context

FIELD TRIPS

Premeeting

Quaternary Sea-level Change and Coastal Evolution in Eastern Maine, *Nov. 1–4*

Rare Element Granitic Pegmatites of Northern New England, *Nov. 2–3*

The Notches: Bedrock and Surficial Geology of New Hampshire's White Mountains, *Nov. 2–4*

The Science Behind *A Civil Action*, *Nov. 3* and *Nov. 4*

The Founders of American Geology: A Visit to their Tombs and Favorite Exposures, *Nov. 3–4*

Geological, Geochemical, and Environmental Aspects of Metamorphosed Black Shales in Maine, *Nov. 3–4*

Avalonian through Alleghanian Tectonism in Southeastern New England, *Nov. 4*

Geochronology and Geochemistry of the Shelburne Falls Arc and the Taconian Orogeny in Western New England, *Nov. 4*

N-Y-F Pegmatites in the Avalon Terrane of Southeastern New England, *Nov. 4*

Quaternary Environments and History of Boston Harbor, Massachusetts, *Nov. 4*

Urban Geology of Beacon Hill and Vicinity, Boston, Massachusetts: In Memory of James V. O'Connor—A Walking Tour, *Nov. 4*

Concurrent

Cobblestones, Puddingstone, and More: Boston's Use of Stone as an Essential Urban Element—A Walking Tour, *Nov. 6*

Engineering Geology of the Big Dig Project (Boston Central Artery Project), *Nov. 7*

Igneous Petrology and Field Relations at Pine Hill, Medford, Massachusetts, *Nov. 6*

Tour of the Salem Harbor Power Plant, *Nov. 6*

Geology of East Point, Nahant, Massachusetts, *Nov. 7*

Geology, Groundwater Contamination, and Groundwater Remediation at the Massachusetts Military Reservation (MMR), Cape Cod, *Nov. 7*

Postmeeting

Deformation, Metamorphism, and Granite Assent in Western Maine, *Nov. 8–11*

Geology of Mount Monadnock, New Hampshire, *Nov. 9*

Geology and Water Supply Development at the Massachusetts Military Reservation (MMR), Cape Cod, *Nov. 9*

MetroWest Water Supply Tunnel Project, *Nov. 9*

Recent Developments in the Study of the Neoproterozoic Boston Bay Group, *Nov. 9*

Metamorphism of a Fold-Thrust Belt in the Hinterland of the Alleghanian Orogen in Southern New England, *Nov. 9–10*

The Taconic Questions: Revisiting the Scenes of the Great American Controversies, *Nov. 9–10*

Prehistoric Bedrock Quarries of the Central Appalachians, *Nov. 9–11*

Zinc and Iron Deposits of the Adirondack Mountains and New Jersey Highlands, *Oct. 30–Nov. 3*

Environmental Geochemistry and Mining History of Massive Sulfide Deposits in the Vermont Copper Belt, *Nov. 8–10*

COURSES/WORKSHOPS/FORUM

Application of Thermochronometry to Tectonics, *Nov. 3–4*

Micromorphology of Glacigenic Sediments, *Nov. 3–4*

Applications of Environmental Isotopes to Watershed Hydrology and Biogeochemistry, *Nov. 4*

Estimating Rates of Groundwater Recharge, *Nov. 4*

Management and Leadership Skills for Geoscience Department Chairs and Institute Directors, *Nov. 4*

Mobilization of Metals from Fossils Fuels: Impacts to the Environment and Human Health, *Nov. 4*

Practical Geoscience Ethics: Elements, Examples, and Education, *Nov. 4*

Tectonics and Topography: Crustal Deformation, Surficial Processes, and Landforms, *Nov. 4*

Sequence Stratigraphy for Graduate Students, *Nov. 3–4*

Stable Isotope Geochemistry, *Nov. 3–4*

Brachiopods, *Nov. 4*

The Art of Technical Writing: Improving Your Technical Reports, *Nov. 4*

Gender Equity Workshop, *Nov. 4*

Girl Scout Geology Badge Workshop, *Nov. 3*

Job Hunting and Career Development Workshop, *Nov. 4*

Practical Application of XRF Techniques to the Analysis of Geological Materials, *Nov. 5*

Digital Forum, *Nov. 7*

Surviving Academia—From Getting the Job to Winning Tenure, *Nov. 4*

Geology, Public Land, and YOU, *Nov. 4*

Exploring the Solar System in the Classroom: A Multisensory Approach, *Nov. 3*

How to Get an Undergraduate Research Program Started, *Nov. 4*

Designing a Successful Student-Centered Online Geology Course, *Nov. 4*

Earth Science Activities to Develop Process Skills of Elementary School Students, *Nov. 3*

Earthquakes—A Workshop for College Faculty, *Nov. 4*

Exploring Plate Tectonics: A Hands-on Approach, *Nov. 4*

Evolution: Investigating the Evidence for Teachers Grades 6 to 16, *Nov. 3*

For more information about the annual meeting, contact GSA, Meetings Dept., P.O. Box 9140, Boulder, CO 80301 • (303) 447-2020 or 1-800-472-1988 • Fax: 303-447-0648 • e-mail: meetings@geosociety.org • World Wide Web: http://www.geosociety.org. *The preregistration deadline is September 28.*

notes on new publications

Relation of Shallow Water Quality in the Central Oklahoma Aquifer to Geology, Soils, and Land Use

USGS Water-Resources Investigations Report 00-4241

As part of the National Water-Quality Assessment Program, the USGS has investigated the effects of geology, soils, and land use of the Central Oklahoma aquifer. The Central Oklahoma aquifer study unit encompasses ~8,000 km^2 of central Oklahoma and comprises several geologic formations, including the Garber Sandstone and Wellington Formation and alluvial deposits. These aquifers are used extensively to supply water for municipal, industrial, commercial, and domestic needs. Several water-quality problems exist in some parts of the aquifer, including elevated concentrations of naturally occurring arsenic, chromium, and selenium that may exceed drinking-water standards. Results of the investigation are presented in this 31-page report by Alan H. Rea, Scott C. Christenson, and William J. Andrews.

Order WRI 00-4241 from: U.S. Geological Survey, Water Resources Division, 202 N.W. 66th St., Bldg. 7, Oklahoma City, OK 73116; phone (405) 843-7570; fax 405-843-7712. A limited number of copies are available free of charge.

Water Chemistry Near the Closed Norman Landfill, Cleveland County, Oklahoma, 1995

USGS Water-Resources Investigations Report 00-4238

The Norman Landfill was selected for study as part of the USGS Toxic Substances Hydrology Program, and a multidisciplinary investigation began in 1994, in collaboration with scientists at the University of Oklahoma, Oklahoma State University, and the U.S. Environmental Protection Agency. The Norman Landfill is located south the City of Norman on alluvial deposits of the Canadian River. Type of waste deposited in the landfill from 1922 to 1973 was largely unrestricted and may include substances now recognized as hazardous. Dissolved and suspended substances leached from wastes in the closed and capped landfill are now in ground water extending toward the Canadian River as a plume of leachate. The results of an initial investigation of the ground- and surface-water chemistry at the site during October through December 1995 are described in this 44-page report by Jamie L. Schlottmann.

Order WRI 00-4238 from: U.S. Geological Survey, Water Resources Division, 202 N.W. 66th St., Bldg. 7, Oklahoma City, OK 73116; phone (405) 843-7570; fax 405-843-7712. A limited number of copies are available free of charge.

Saline Contamination of Soil and Water on Pawnee Tribal Trust Land, Eastern Payne County, Oklahoma

USGS Water-Resources Investigations Report 00-4271

Using hydrogen and oxygen isotopes, water-quality data, and surface and borehole geophysics, the U.S. Geological Survey found evidence that brine water contaminated soil and surface and ground water around abandoned oil production equipment on Pawnee tribal trust land near Yale, Oklahoma. The USGS, in cooperation with the Bureau of Land Management, inititated the investigation in March 1998 to determine the extent of surface contamination, possible sources of surface- and ground-water contamination, and saline contamination of the Ada Group, the shallowest freshwater aquifer in the area. The results are described in this report by Donna Runkle, Marvin M. Abbott, and Jeffrey E. Lucius.

Order WRI 00-4271 from: U.S. Geological Survey, Water Resources Division, 202 N.W. 66th St., Bldg. 7, Oklahoma City, OK 73116; phone (405) 843-7570; fax 405-843-7712. A limited number of copies are available free of charge.

Hydrogeologic Report of the El Reno, Fairview, Isabella, and Loyal Minor Groundwater Basins in Central Oklahoma

OWRB Technical Report 2000-1

This report contains information on each basin's physical setting, descriptions of the aquifer parameters, storage and yield capabilities, water use and prior ground-water rights, color maps, and analyses of water quality. Mark Belden wrote the report, with support from Noel Osborn and Bob Fabian.

Order OWRB Technical Report 2000-1 from: Oklahoma Water Resources Board, phone (405) 530-8800. The report costs $5.

Oklahoma abstracts

The Oklahoma Geological Survey thanks the American Association of Petroleum Geologists and Geological Society of America for permission to reprint the following abstracts of interest to Oklahoma geologists.

Seismic Ray-Trace Modeling as a Tool for Interpreting Complex Subsurface Structures in the Wichita Mountains Frontal Zone, Southern Oklahoma

JAN M. DODSON, KEVIN J. SMART, and *ROGER A. YOUNG,* School of Geology and Geophysics, University of Oklahoma, Norman, OK 73019

The Wichita Mountains Frontal Zone (WMFZ) is part of the linear trend in southern Oklahoma that extends from the Arbuckle Mountains in south-central Oklahoma through the Wichita Mountains to the buried Amarillo Mountains in the Texas Panhandle. Intense subsurface deformation exists along the WMFZ, including overturned beds and crystalline basement rocks thrust over Paleozoic sedimentary rocks. Correct migrations of seismic data are vital to accurate interpretations; but they cannot be achieved without well-defined velocity models. Velocity models are in turn based on interpretations of the data. Seismic ray-tracing can confirm or condemn an interpretation.

A synthetic zero offset seismic data set paralleling an actual seismic line was created with ray-tracing software by building a valid cross section using all available data, including well data and seismic data. Ray paths were calculated and analyzed to determine where reflections occurred in the subsurface and their corresponding CMP location. Arrival times and reflection amplitudes were used to produce synthetic traces for comparison to actual seismic data.

Two alternate velocity models were constructed to demonstrate that a lack of data, or an inaccurate interpretation, produce ambiguous results. The synthetic data set was time migrated with the exact velocity grid used to create the data; then the data set was migrated with the alternate velocity models. Comparing the three resulting migrations to the actual seismic data confirmed that the more accurate migration velocity model produced the clearest result. The most accurate migration, however, does not accurately position all reflection events. A reflection from the overturned limb of an anticline is not placed in the correct horizontal location.

Reprinted as published in the Geological Society of America *2001 Abstracts with Programs*, v. 33. no. 5, p. A-45.

Last Tectonic Signal from ARM's Wichita-Amarillo Block is Recorded by Permian Post Oak Conglomerate and Paleotopography

M. C. GILBERT, School of Geology and Geophysics, University of Oklahoma, Norman, OK 73019

The Wichita-Amarillo and Arbuckle crustal blocks are fartherest east of the Ancestral Rocky Mountains (ARM). The Wichita Mountains of southwestern Oklahoma, and part of the Arbuckle Mountains of southern Oklahoma, are the surface expression of the Cambrian Southern Oklahoma Aulacogen. This rift zone was uplifted as discrete crustal blocks in the Pennsylvanian, recognized by many as beginning in the Morrowan, through sedimentological signals in units in adjacent Anadarko and related basins (~330 Ma). Timing and nature of the last tectonic signal in the Wichita-Amarillo block, and thus length of tectonism, have not been much emphasized. End of tectonism for this block is recorded by the Permian (Leonardian) Post Oak Conglomerate, a facies of the Garber Sandstone–Hennessey Group (~270 Ma).

The Post Oak was recognized as a distinct stratigraphic unit by Chase in 1954, with 3 distinct facies: granite clast, rhyolite clast, and limestone clast types, reflecting local sources. The characteristically rounded granitic clasts formed through spheroidal weathering in an interval of tectonic quiescence, allowing widespread low-relief landscapes and deep weathering, just preceding final uplift. Then a concentrated period of uplift, where erosion rates greatly exceeded weathering rates, dismantled the deep regolith of active spheroidal weathering, and distributed the corestones and finer debris as sedimentary aprons around the newly uplifted, less-weathered bedrock. Maximum thickness of the Post Oak provides a minimum estimate of the amount of vertical uplift: <100 m. However, relief of the Permian topography, formed during this uplift and subsequently buried and preserved by the Hennessey shales, gives a better estimate: 300–400 m. Donovan used different arguments, relating to lateral offsets of the limestone clast facies, to give potential strike-slips of several km.

Thus, while final ARM tectonism in this block yielded offsets 1–2 orders of magnitude less than that "forming" the blocks at the beginning of uplift, the end and last stage of tectonism, approximately 60 Ma later, was still significant.

Reprinted as published in the Geological Society of America *2001 Abstracts with Programs*, v. 33. no. 5, p. A-46.

Anatomy of an A-Type Cambrian Felsic Volcanic Field: Carlton Rhyolite in the Blue Creek Canyon Area, Wichita Mountains, Southern Oklahoma

CHRISTINE M. PHILIPS and *RICHARD E. HANSON,* Dept. of Geology, Texas Christian University, TCU Box 298830, Fort Worth, TX 76129

The Carlton Rhyolite is an extensive A-type felsic extrusive unit occurring at the top of a suite of rift-related Cambrian igneous rocks in the Southern Oklahoma aulacogen. The rhyolite is quite extensive in the subsurface but crops out only in limited areas in the Wichita and Arbuckle Mountains. The Blue Creek Canyon area in the Wichita Mountains contains some of the best exposures of the rhyolite but has received little previous study. A minimum stratigraphic thickness of 800 m of rhyolite is present in the area; the base is not exposed and the top is overlain unconformably by Upper Cambrian strata. Detailed

mapping has identified at least five major flow units ranging from 160 to 190 m in thickness. These extend laterally for greater than 3 km and appear to be tabular. Most flow boundaries are locally defined by peperites or bedded tuffaceous deposits 8–30 cm thick. Limited sediment accumulation between flows implies rapid eruption of a series of flow units in a narrow time frame. The peperites formed when rhyolite flowed over wet sediments deposited between eruptions and consist of angular clasts or irregular globs of rhyolite set in a matrix of disrupted tuff. The flows consist dominantly of lithoidal, nonvesicular rhyolite, but finely flow-laminated glass (now devitrified and preferentially altered) with relict perlitic texture forms zones up to 35 m thick along the upper and lower flow margins. A distinct zone up to 5 m thick rich in lithophysae occurs inward from the chilled margins. These regular vertical textural changes indicate that each flow is a single cooling unit. No textural evidence for a pyroclastic origin for any of the flows has yet been found, implying that they are not rheomorphic ignimbrites and instead may represent flood rhyolites produced by effusion of relatively low-viscosity, high-T, A-type magmas.

Reprinted as published in the Geological Society of America *2001 Abstracts with Programs*, v. 33. no. 5, p. A-24.

Geophysical Evidence for Magmatic Modification of the Crust in the Rocky Mountain Region

G. RANDY KELLER, CATHERINE SNELSON, KATE C. MILLER, and *OSCAR QUEZADA*, Dept. of Geological Sciences, University of Texas at El Paso, El Paso, TX 79968

A variety of recent geophysical studies document that magmatic modification of the crust in the Rocky Mountain region has been widespread and locally extensive. The initial accretionary events that formed the crust were accompanied by intrusion (~1.6 Ga). The crust then experienced intrusion and burial by huge volumes of granitic and rhyolitic rocks 1.4–1.3 Ga. Regional extension and mafic magmatism occurred at ~1.1 Ga, contemporaneous with the Grenville orogeny that completed the formation of the supercontinent in this region. Coincident, short wave-length gravity and magnetic anomalies delineate mafic intrusions in the upper crust of a variety of ages with 1.1 Ga probably being the main period of intrusion. The break-up of Rodinia that followed soon thereafter involved considerable magmatism with the massive upper crustal mafic complex in the Southern Oklahoma aulacogen being the best example. Felsic intrusions are harder to delineate, because the negative gravity anomalies they cause can be indistinguishable from those caused by sedimentary basins. This effect is well documented in the Taos-Mora area where a ~1.6 Ga intrusion and Phanerozoic sediments combine to produce a prominent gravity low. The Mid-Tertiary batholithic intrusions associated with the Datil-Mogollon and San Juan volcanic fields produce intense gravity lows that are evidence of large scale modification of the upper crust. The Valles caldera certainly represents significant magmatic modification of the crust, but not at the scale of these features. From a deeper crustal point of view, the origin of the underplated (?), high velocity lower crust is a major question. The massive amount of 1.4 Ga magmatism in the upper crust suggests a causal relationship, but this hypothesis needs much more documentation and testing.

Reprinted as published in the Geological Society of America *2001 Abstracts with Programs*, v. 33. no. 5, p. A-50.

The Early Mississippian Sycamore Formation in the Arbuckle Mountains, Southern Oklahoma

R. NOWELL DONOVAN, Dept. of Geology, Texas Christian University, TCU Box 298830, Fort Worth, TX 76129

The early Mississippian Sycamore Formation records the beginning of crustal mobility that marked the closure of the Laurentian and Gondwana Plates. A tectonic framework, involving localized basin and uplift, developed from the beginning of Sycamore times. The Formation, which is 250–350 ft thick, ranges in age from Kinderhookian to earliest Meramecian. It conformably overlies the upper Devonian Woodford Formation and unconformably underlies the Mississippian Caney Shales. A lower "Transition" member is composed of grey shales and argillaceous cherty limestones; an upper member consists of grey shales and tan-weathering marlstones containing up to 50% silt-sized siliciclastic grains. The shales record slow deposition in a "deep" water setting. Individual marlstone beds display a sharp or erosive base and a massive basal layer from a few inches to four feet thick. Other features include, in the uppermost part of some beds, horizontal lamination, low amplitude ripple marks and horizontal burrows. Thin lags of fossil hash occur at the base of some beds. These beds are interpreted as turbidites that reworked fine-grained distal shelf material into a hierarchical arrangement of fan packages. The near absence of typical Bouma profiles is a reflection of the fine-grained nature of the available sediment. Current movement was to the west. Well-exposed sections on I-35, located 7 miles apart on the limbs of the Arbuckle anticline, display similar, but not identical sequences. The northern section displays features that suggest it was located closer to source than the southern; this relationship can be extended to the "Transition" member where a shelf carbonate—the Welden Limestone—is represented to the south by "deep" water bedded chert and calcareous shale.

Reprinted as published in the Geological Society of America *2001 Abstracts with Programs*, v. 33. no. 5, p. A-47.

Diabase Dikes, Eastern Arbuckle Mountains, Oklahoma: Two Magmatic Suites and Regional Implications

EDWARD G. LIDIAK, Dept. of Geology and Planetary Science, University of Pittsburgh, Pittsburgh, PA 15260; and *RODGER E. DENISON*, Dept. of Geosciences, University of Texas at Dallas, Richardson, TX 75083

Numerous northwest-striking diabase dikes cut massive 1350–1400 Ma granitic rocks in the eastern Arbuckle Mountains. Most of the dikes were apparently emplaced during Early Cambrian rifting that resulted in the formation of the Southern Oklahoma aulacogen. Whole rock K-Ar results suggest some of these dikes are older and may be near the age of the host granitic rocks. However, there is no petrographic difference in the dikes, and the K-Ar isotopic system is plagued by excess radiogenic argon.

Detailed trace element and Nd and Sr isotope geochemistry reveal that there are two distinct suites of diabase dikes. Compared to the apparently older dike set, the younger dikes are characterized by lower Mg number, by greater abundances of incompatible elements such as K, Ti, P, Y, Zr, Nb, Ta, Th, and by light and medium rare earths. The younger dikes also have higher initial Sr and lower initial Nd isotopic ratios.

Diabasic dikes are common throughout the widespread granite-rhyolite terranes in the Proterozoic basement of central United States. These dikes record extensional events and probably play a major role as seismic reflectors that help define the thickness and extent of the separate terranes. The early northwest-striking diabase dikes in the eastern Arbuckle Mountains may record an extensional event that led to the formation and preservation of the enigmatic 10-km-thick layered Precambrian reflections in southwest Oklahoma and adjacent Texas. A direct relationship is now obscured by Cambrian and later rifting that separates them.

Reprinted as published in the Geological Society of America *2001 Abstracts with Programs*, v. 33. no. 4, p. A-19.

Overview of the Southern Oklahoma Aulacogen

M. C. GILBERT, School of Geology and Geophysics, University of Oklahoma, Norman, OK 73019

The Southern Oklahoma Aulacogen (SOA) represents the last magmatic episode of the crustal block known as Laurentia. Understanding its magmatic/tectonic history, and the origin of its rocks, may contribute to an understanding of the formation of other rifts which have cut Laurentia and the nature of the subjacent mantle. Some key points: (1) Age, as dated by its exposed parts, is 530–540 Ma, near the Proterozoic–Cambrian boundary. (2) The SOA now is a fin of mantle-derived material cross-cutting presumed older Granite-Rhyolite crust. (3) The SOA represented an intimate connection between magmatism and extensional tectonism. (4) The exposed silicic parts represent the top of the rift sequence. Most of the buried SOA additions to the crust are mafic. (5) The extent of the SOA is outlined in the positive Bouguer gravity anomaly in the regional gravity field. (6) The SE end of the SOA marks the southern edge of Laurentia. (7) The SOA crustal section behaved mechanically as a unit in subsequent tectonism, dismembering the ancestral Anadarko (Oklahoma) Basin during the Pennsylvanian Ouachita orogeny.

The relations known and reasonably inferred for this rift may be used as a reference for comparing other buried and less completely exposed rifts of southern Laurentia.

Reprinted as published in the Geological Society of America *2001 Abstracts with Programs*, v. 33. no. 4, p. A-42–A-43.

Paleoproterozoic and Mesoproterozoic Domains Within the Southern Granite-Rhyolite Province Identified Using Sm-Nd Isotopic Methods

C. R. ROHS, Dept. of Geology and Geography, Northwest Missouri State University, Maryville, MO 64468; and *W. R. VAN SCHMUS*, Dept. of Geology, University of Kansas, Lawrence, KS 66045

In the midcontinent of North America, large areas of the Precambrian basement formed during the Proterozoic. This study presents new information about the temporal framework and tectonic processes indicated by rock samples associated with the Southern Granite-Rhyolite (SGR) province. The purpose of this research was to examine basement samples within the southern midcontinent in order to refine the limits and properties of individual crustal domains. Previous studies have shown that crustal residence ages, as determined by Sm-Nd isotopic analysis, typically decrease to the south and east. More than sixty whole-rock samples were analyzed for crustal residence ages as part of this study. These samples also indicated a trend in the crustal residence ages decreasing to the south and east. Four crustal domains have been identified in the SGR province using the new isotopic data along with previous isotopic data, rock descriptions, and geochemical data. Two of the domains, the Panhandle and Eastern Domains, have crustal residence ages >1.55 Ga indicating the presence of Paleoproterozoic crust below the SGR province. The other two domains, the Arbuckle and Crystalline Domains, have crustal residence ages <1.55 Ga and have been interpreted as underlain by Mesoproterozoic crust. The tectonic interpretation of this data focuses on the growth of the continent during the Proterozoic including accretion of arc terranes, crustal growth at the continental margin, and widespread extension.

Reprinted as published in the Geological Society of America *2001 Abstracts with Programs*, v. 33. no. 4, p. A-10.

Models for the Origin of the Mesoproterozoic "Granite-Rhyolite" Province

ROBERT D. SHUSTER, Dept. of Geography and Geology, University of Nebraska, Omaha, NE 68182

The Mesoproterozoic Granite-Rhyolite Province underlies much of the midcontinent of North America and ranges in age from 1.5 to 1.3 Ga old. In general, older parts of this province (1.5–1.4 Ga old) occur in the east and younger (1.4–1.3 Ga old) examples are more common in the southern and western parts of the province. This province is composed primarily of undeformed high silica rhyolites and related epizonal granitic plutons. Igneous rocks of intermediate and mafic compositions are volumetrically rare.

These rocks have been traditionally referred to as being "anorogenic," based on several factors. There is a lack of widespread deformation in the rocks, the igneous rocks are not calc-alkaline, and the types of metamorphic and sedimentary rocks associated with convergent or divergent plate boundaries today are mostly missing. Also, the granites have been classified as having an A-type geochemical signature. Geochemical data collected on a suite of these rocks suggest a source region that was heterogeneous in composition and age, although there is little evidence of contribution of any Archean crust to the source region(s) of these granites and rhyolites.

Potential models for the origin of this province will be discussed. These will include the possibility of the Granite-Rhyolite Province being a Large Igneous Province and what role subcrustal lithospheric delamination may have played in this widespread and relatively long-lived magmatic event.

Reprinted as published in the Geological Society of America *2001 Abstracts with Programs*, v. 33. no. 4, p. A-10.

Bryozoan Species in the Chickasaw Bryozoan Reef (Ordovician, Oklahoma)

SCOTT P. WERTS, *ROGER J. CUFFEY*, and *CLIFFORD A. CUFFEY*, Dept. of Geosciences, Pennsylvania State University, University Park, PA 16802

For the first time, bryozoan species composition of a mid-Ordovician bryozoan reef far outside the Appalachians has been analyzed, thereby permitting informative comparisons with other such structures of comparable age. We identified 120 colonies from different ecozones in the Chickasaw bryoherm (Cuffey and Cuffey, 1995), of basal Blackriveran age

(low in Mountain Lake Member of Bromide Formation), on U.S. Hwy. 177 1.4 mi (2.3 km) SE of the center of Sulphur in south-central Oklahoma.

The micritic cruststone core of the Chickasaw bryozoan reef contains all the species identified in and around this small bioherm. Crustose to massive *Batostoma chazyensis* (incl. *campensis*) and *Dianulites fastigiatus* are abundant, *Lunaferamita* (*Fistulipora*) *bassleri* common, and *Tarphophragma* (*Hallopora*) *multitabulata* and bifoliate *Escharopora recta* sparse. Broken fragments of these also occur scattered through the calcarenitic packstone flank beds.

Seventeen additional species are rare in the core (some also rare in the crinoidal grainstones underlying [*] or overlying [**] the reef). Many are similar trepostomes: *Batostoma ramosa, sheldonensis, Dianulites petropolitana**, *Diplotrypa bassleri, Homotrypa dickeyvillensis**, *tuberculata, Mesotrypa angularis, Nicholsonella acanthobscura, Orbignyella sublamellosa*; a few, cystoporates: *Ceramoporella ingenua, Lunaferamita virginiensis.* Some are thin-branching trepostomes: *Champlainopora* (*Atactotoechus*) *chazyensis**, **, and *Batostomella* (*Bythopora*) *subgracilis*; or bifoliates: *Graptodictya* (*Stictopora*) *elegantula, Graptodictya* (*Arthropora*) *simplex, Pachydictya* (*Athrophragma*) *sheldonensis**, *Stictopora* (*Rhinidictya*) *fenestrata.*

Most of these species functioned as encrusting frame-builders, sometimes eroded off the reef to form skeletal grains. The more delicate trepostomes and bifoliates grew like sparse grass across the mound surface.

The Chickasaw reef contains the greatest concentration of bryozoan species (21) identified in the immediate area. This bryodiversity is noticeably higher than the somewhat older Vermont Chazyan bryoherms (particularly the earliest one, at Garden Island), but is comparable to other crust-mounds of similar Blackriveran age (Tennessee, Virginia). Moreover, the proportion of abundant to rare species suggests fossilization in place with little if any taphonomic alteration.

Reprinted as published in the Geological Society of America *2001 Abstracts with Programs*, v. 33. no. 5, p. A-54–A-55.

Sustaining Aquifer Discharge as a Cultural and Historic Resource

MICHAEL NICHOLL, Dept. of Materials, Metallurgical, Mining, and Geological Engineering, University of Idaho, Moscow, ID 83844; and *JASON NORD*, School of Geology, Oklahoma State University, Stillwater, OK 74078

The Arbuckle-Simpson Aquifer is a productive sequence of fractured carbonate units located in south-central Oklahoma. Discharge from this artesian aquifer supplies springs and streams in Chickasaw National Recreation Area (CNRA); an entity that was originally established in 1902 as the Sulphur Springs Reservation in order to protect a 640-acre tract containing more than 30 fresh and mineralized cold springs. Water from many of these springs was reputed to possess significant medicinal value, and hence consumed for a variety of ailments. Over the intervening years, spring flow has declined significantly, and many of the springs have ceased to flow. The problem of sustaining and restoring natural spring flow is complicated by a lack of geologic information, competing uses, and a fundamental lack of knowledge regarding flow through fractured aquifers. In order to help understand the local flow system, a constant drawdown test was performed on a 775-foot-deep artesian well flowing at a nominal rate of ~620 gallons per minute. Recovery to nominal flow was extremely rapid (<3 minutes), confirming our a priori expectation of a highly transmissive fractured unit exhibiting little storage.

Reprinted as published in the Geological Society of America *2000 Abstracts with Programs*, v. 32, no. 7, p. A-141.

Distributary Channels, Fluvial Channels or Incised Valleys?

JANOK P. BHATTACHARYA, A. ROBINSON, C. OLARIU, M. M. ADAMS, C. D. HOWELL, and *R. M. CORBEANU,* University of Texas at Dallas, Richardson, TX 75083

Many deltas show several orders of branching resulting in a wide range of sizes and shapes of distributary channels. There is thus no such thing as "a distributary channel" in many deltas. At the largest scale, trunk rivers become distributive at the point where the river becomes unconfined (nodal avulsion). Intermediate-scale delta plain channels tend to be few in number, may be separated by wide interfluves, and may be exceedingly difficult to distinguish from fluvial channels. The smallest scale "terminal distributaries" lie in the delta front. Because discharge decreases downstream, terminal distributary channels tend to be narrow and shallow, rather than wide and deep.

In many mid-continent reservoirs, such as the Pennsylvanian Booch sandstone in Oklahoma, 100-m-thick channelized deposits cut into 10-m-thick prodelta and delta front deposits, but have been historically interpreted as distributary channels. These interpretations were strongly driven by using the deep distributary channels of the Mississippi delta as a modern analog, which is probably not appropriate because it feeds into deep water, rather than an interior sea. These deeply incised channels might be better interpreted as multi-storey incised valleys rather than single-storey distributary channels.

Outcrop examples of terminal distributary channels in the Cretaceous Panther Tongue sandstone in Utah show multiple, shallow channelized sandstones, intimately associated with more extensive delta front clinoform beds. These better match modern shoal-water deltas such as the Atchafalaya delta in the Gulf Coast.

Reprinted as published in the American Association of Petroleum Geologists *Bulletin*, v. 85, p. 384, February 2001.

Temporal Benchmarks for Modeling Phanerozoic Flow of Basinal Brines and Hydrocarbons in the Southern Midcontinent Based on Radiometrically Dated Calcite

RAYMOND M. COVENEY, JR., University of Missouri, Kansas City, MO 64110; *VIRGINIA M. RAGAN*, Maple Woods Community College, Kansas City, MO 64156; and *JOYCE C. BRANNON*, Washington University, St. Louis, MO 63130

Fluid-inclusion studies of radiometrically dated (U/Pb, Th/Pb) calcite samples document the presence of hydrothermal fluids at ca. 251, 137, 67, and probably 39 Ma within the Tri-State Zn-Pb mining district of Missouri, Kansas, and Oklahoma. Fluid inclusions indicate minimum temperatures and equivalent salinities ranging from highs of 122°C and 24 wt% NaCl ca. 251 Ma to lows of 52°C and 0 wt% NaCl ca. 39 Ma. The two earliest calcites contain primary petroleum inclusions, but these are absent in samples younger than ca. 137 Ma. When combined with information on metal-rich shales, paleomagnetism,

and modern groundwater flow, our results are most readily explained by periodic influxes of hydrothermal fluids of diverse compositions for >200 m.y. and sporadic migration of hydrocarbons for at least 100 m.y. in the southern Midcontinent.

Reprinted as published in *Geology*, v. 28, p. 795, September 2000.

Mobility of Rare-Earth Elements (REE) in Marine Carboniferous Phosphates and Host Shales from the Midcontinent and Implications for Shale Provenance Analysis

DAVID L. KIDDER, Dept. of Geological Sciences, Ohio University, Athens, OH 45701; *RAMA KRISHNASWAMY*, Dept. of Geological Sciences, George Washington University, Washington, DC 20052; and *ROYAL H. MAPES*, Dept. of Geology, Ohio University, Athens, OH 45701

The nature and extent of diagenetic movement of middle rare-earth elements (MREE) to phosphate nodules from pore waters of host muds can help determine the reliability of geochemical provenance analysis in shales. Paired analyses of phosphate concretions and black and gray host shales from the Eudora, Muncie Creek, and Stark Shales of eastern Kansas show that the phosphates are MREE-enriched and the host shales are MREE-depleted. Phosphate nodules from other Upper Carboniferous units in Kansas, Oklahoma, Iowa, and Ohio generally display either flat or MREE-enriched patterns with occasional cerium depletions. Other host shales most commonly display flat REE patterns. Cerium depletions in all three laminar phosphate samples from Nebraska suggest that genesis of phosphatic laminae was influenced by overlying seawater.

All of the MREE enrichment and depletion patterns are from outcrop samples, yet they are generally comparable to recent results from similar facies in core samples analyzed by Cruse et al. (2000). Although black shales are susceptible to chemical weathering, the similar chemistry between outcrop and core results suggests that the samples in our data set were not significantly altered by weathering.

The REE mobility discussed above appears consistent with movement of other elements used in provenance analysis. Preliminary results suggest that the chemistry of shale samples in which MREE have moved from host mud to phosphate differs from shales with flat REE patterns that presumably reflect less elemental migration. Ratios of Fe2O3/TiO2, Al2O/(Al2O3 + Fe2O3), and values of La and Sc all appear to be grouped according to REE pattern. Shales with flat REE patterns are probably more reliable choices for provenance analysis than those in which REE have moved.

Reprinted as published in the Geological Society of America *2001 Abstracts with Programs*, v. 33. no. 5, p. A-22.

Rare-Earth and Trace Element Analysis of Biogenic (Conodont) Apatite: Dennis and Swope Formations, Upper Pennsylvanian (Missourian), Midcontinent, USA

CAMOMILIA ANISE BRIGHT, TIMOTHY W. LYONS, RAYMOND L. ETHINGTON, and *MICHAEL D. GLASCOCK*, University of Missouri, Columbia, MO 65211

Pennsylvanian strata of midcontinent North America are characterized by cyclic deposits of inferred glacioeustatic origin. The classic cyclothem spans from nearshore siliciclastics to limestone to offshore euxinic shale. Conodonts from this full range of facies were collected in two Missourian cyclothems, the Swope and Dennis formations of Iowa, Missouri, Kansas, and Oklahoma, and were analyzed for rare-earth element (REE) and trace element (TE) contents. Data were generated with a threefold agenda: (1) to characterize local and global ocean chemistry as expressed in a dynamic paleoepicratonic seaway; (2) to use stratigraphic and spatial trends to better constrain the mechanisms that drove cyclic deposition; and (3) to test new approaches to conodont geochemistry and the reliability of preserved primary records relative to diagenetic overprints, including apatite oxygen isotope data.

Preliminary results generated by UV laser ablation coupled to a high-resolution Inductively Coupled Plasma Mass Spectrometer suggest that REE and TE variation may be significant within individual conodont elements. Such small-scale heterogeneities argue against wholesale diagenetic resetting. To test the extent to which biogenic apatite undergoes alteration during diagenesis and the potential for recording primary (water-column) variation that occurred during the life span of a given individual, growth lamellae within single conodont platform elements will be analyzed by laser for REE and TE concentrations. Geochemical analyses of conodonts have traditionally been performed using taxonomically mixed bulk samples, which limits geochemical resolution. By contrast, analysis of individual conodonts will permit intrageneric comparisons among a variety of localities and stratigraphic intervals. Such comparisons should illuminate temporal and regional variability in midcontinent ocean chemistry during the Pennsylvanian. Furthermore, intergeneric REE and TE variation in a given stratigraphic horizon may reflect vertical chemical gradients within the ancient water column. More broadly, this presentation is a progress report of approaches to conodont chemostratigraphy.

Reprinted as published in the Geological Society of America *2001 Abstracts with Programs*, v. 33. no. 4, p. A-21–A-22.

Upper Mississippian (Chester) Ooid Shoals: Austin Upper Mississippian Field, New Mexico, and Mocane-Laverne Field, Oklahoma, and their Relation to North American Chester Paleogeography

D. C. HAMILTON, Independent, Midland, TX; and *G. B. ASQUITH*, Texas Tech University, Lubbock, TX 79409

Upper Chester ooid grainstones produce gas in both the Austin Upper Mississippian field in Lea County, New Mexico (13 BCF + 130 MBO) and the Mocane-Laverne field in Harper and Beaver counties, Oklahoma (703 BCF). These ooid grainstones were deposited in an upper Chester HST due to a loss of accommodation space. The reservoirs in both fields are skeletal ooid grainstones with intergranular porosity.

The ooid grainstones in southeast New Mexico were deposited as a series of northeast–southwest-trending elongate ooid shoals perpendicular to the Chester shelf margin. In the Mocane-Laverne field in northwest Oklahoma the Chester ooid shoals exhibit a similar geometry, but are oriented northwest–southeast also perpendicular to the Chester shelf margin. The orientation of the Chester ooid shoals perpendicular to the shelf margin is similar to the orientation of modern ooid tidal bar belts at the end of the Tongue of the Ocean in the Bahamas. Chester ooid grainstones have also been reported in southwest New Mexico, West Texas, north-central Texas, southwest Kansas, and north-central Arkansas plus the Illinois and Appalachian basins. Therefore, south of the Mississippian paleo-

equator Chester ooid shoals may have extended across southern New Mexico around the Texas Peninsula into Oklahoma across to Arkansas all the way to the Appalachian Basin; deposited along the upper Mississippian shelf margin a distance of over 2,600 miles.

Reprinted as published in the American Association of Petroleum Geologists *Bulletin*, v. 85, p. 386, February 2001.

Petrography and Permeability of the Mesa Rica Sandstone at Autograph Rock, Oklahoma

RAY KENNY and *HEATHER LANCOUR*, Environmental Geology Program, New Mexico Highlands University, P.O. Box 9000, Las Vegas, NM 87701

A reconnaissance field and laboratory study was conducted to determine the petrography and permeability of the sandstone exposed at Autograph Rock, OK. Autograph Rock is a 30-ft-high cliff along Cold Springs Creek that hosts over 200 inscriptions dating from 1850. The historic inscriptions are carved into the (100–110 Ma) Mesa Rica Sandstone (Dakota Group). Autograph Rock was an important stop along the Santa Fe Trail because of the excellent and dependable water supply at this location. The Mesa Rica Sandstone is a quartz-rich sandstone characterized by numerous small-scale cross-stratification sets. Petrographic analysis indicates that the Mesa Rica Sandstone at Autograph Rock is very porous and poorly cemented. Modern weathering of the sandstone at Autograph Rock is due to both biogeophysical and biogeochemical weathering. Much of the disintegration of the sandstone can be attributed to the influence of lichens. The lichens readily penetrate the sandstone, locally increase permeability, and contribute to enhanced weathering and degradation of the sandstone and the inscriptions. The presence or absence of lichens seems to be the most important biogeochemical weathering factor affecting the inscriptions. A mini-permeameter was used to characterize and quantify the permeability of the Mesa Rica Sandstone at Autograph Rock. Preliminary results from the permeameter field study indicate that the lichen-free, cross-bedded sandstone exposures have similar permeability values (excluding concretions, subaerial exposure planes, iron oxide diffusion rings, and certain other variant bedding features); data from lichen-covered exposures indicate increased permeability. This increase in permeability is likely due to increased subsurface fungal penetration. The lichen-covered inscriptions and rock surfaces are therefore subject to a higher degree of degradation relative to lichen-free surfaces.

Reprinted as published in the Geological Society of America *2001 Abstracts with Programs*, v. 33. no. 5, p. A-53.

Rates of Anaerobic Methane Oxidation in a Landfill-Leachate Plume

ETHAN L. GROSSMAN, Dept. of Geology and Geophysics, Texas A&M University, College Station, TX 77843; *LUIS CIFUENTES*, Dept. of Oceanography, Texas A&M University, College Station, TX 77843; and *ISABELLE M. COZARELLI*, U.S. Geological Survey, 431 National Center, Reston, VA 20192

Numerous studies have examined natural attenuation of landfill methane by aerobic oxidation in landfill cover soils, but few have examined attenuation of landfill methane in anaerobic aquifer systems. The alluvial aquifer adjacent to Norman landfill in Oklahoma provides an excellent laboratory for the study of anaerobic methane oxidation in a landfill-leachate contaminated aquifer. As part of a joint study with the U.S. Geological Survey, we collected groundwaters from a transect of seven multilevel wells ranging in depth from 1.3 to 11 m and oriented parallel to the flow path. The leachate plume is characterized by high total dissolved organic carbon, ammonia, ferrous iron, and methane concentrations, and low sulfate concentrations.

Methane concentrations and 13C contents clearly show evidence for methane oxidation within the anaerobic plume and its margins. Methane oxidation causes Δ13C values to increase from about –55 per mil near the source to >–10 per mil at the plume margins and distal end. The carbon isotopic fractionation associated with this methane oxidation is about –18 per mil, with the lighter isotope preferentially incorporated into CO2. We used this isotopic enrichment factor in a Rayleigh distillation model to estimate methane consumption from methane 13C measurements. These calculations show that 80 to 90% of the landfill methane is oxidized over the 210-m transect. Given an average flow rate of 15 m/y, this methane consumption occurs within 14 years. Rate constants for methane oxidation assuming first order kinetics, increase from 0.05 per year for the first 100 m to 0.15 per year for the second 100 m. Oxidation rates vary with methane concentration and distance, but are on the order of 50 uM/y. Rates of sulfate reduction for sediments from within the plume are relatively high (1 mM/y), suggesting that methane oxidation may be mediated by a sulfate reducer-methanogen consortium. Our results demonstrate that anaerobic methane oxidation can be an important mechanism for the natural attenuation of landfill methane in aquifer systems.

Reprinted as published in the Geological Society of America *2000 Abstracts with Programs*, v. 32, no. 7, p. A-127.

The Impact of Sediment-Bound Sulfate and Ferric Iron on Degrading Organic Contaminants in a Leachate Plume at the Norman Landfill, Oklahoma

MICHELE L. TUTTLE and *G. N. BREIT*, U.S. Geological Survey, Box 25046, MS973, Denver, CO; *I. M. COZZARELLI*, U.S. Geological Survey, Reston, VA; and *S. H. HARRIS*, University of Oklahoma, Norman, OK 73019

Sediment-bound sulfate and ferric iron are proposed electron acceptors in the bacterial degradation of organic contaminants (DOC to 200 mg/L) in a groundwater leachate plume from a closed municipal landfill, Norman, Oklahoma. We characterize sulfate and ferric iron in Canadian River alluvium variably affected by the landfill leachate and estimated the impact these electron acceptors have on organic degradation.

Five cores and adjacent wells located up to 400 m from the landfill were sampled. Mud samples contain more total sulfur (avg. 0.14 wt.%) than the sand (avg. 0.02 wt.%) but no systematic differences were detected between background and contaminated sediments. Iron sulfides are the dominant sulfur form. Acid-soluble sulfate was detected only in mud samples (avg. 0.02 wt.%). The groundwater concentration of sulfate was markedly lower in the leachate (<0.05 mM) relative to background groundwater (up to 5 mM). The sulfur isotopic composition of dissolved sulfate is consistent with bacterial reduction except for samples from sand >3 feet thick that has been ex-

posed to leachate for >5 years. The isotopic composition of these samples was similar to background sulfate (10 per mil) and is attributed to the dissolution of detrital barite. The distribution of sulfate-reducing bacteria was estimated using sulfur-35 imaging. Results indicate no activity in mud, spotty activity in sands, and peak activity near sand/mud contacts. The higher activity near sand/mud contacts may be related to sulfate diffusion from mud.

Rapidly reducible ferric iron (RRFe) (0.5 N HCl soluble) up to 0.25 micromoles/g was detected only in background and recently contaminated sediments. More slowly reducible iron (SRFe) (hematite) was estimated using a Ti3+/EDTA extraction. Sand contains about 5 micromoles/g and mud approximately 35 micromoles/g of SRFe, with no significant differences between background and contaminated sites. Apparently, SRFE abundance has not been modified by the leachate.

Sulfate and ferric iron are present in the alluvium but their bioavailability is limited by low abundance, form, and accessibility. Organic degradation supported by solid phase electron acceptors in the alluvium is likely to be slow relative to flow rates within sand intervals.

Reprinted as published in the Geological Society of America *2000 Abstracts with Programs*, v. 32, no. 7, p. A-127.

Geochemical and Microbiological Methods for Evaluating Anaerobic Processes in an Aquifer Contaminated by Landfill Leachate

ISABELLE M. COZZARELLI, U.S. Geological Survey, 431 National Center, Reston, VA 20192; *J. M. SUFLITA, G. A. ULRICH*, and *S. H. HARRIS*, Dept. of Botany and Microbiology, University of Oklahoma, Norman, OK 73019; *R. P. EGANHOUSE* and *M. A. SCHOLL*, U.S. Geological Survey, 431 National Center, Reston, VA 20192; *J. L. SCHLOTTMANN* and *S. C. CHRISTENSON*, U.S. Geological Survey, Water Resources Division, 202 N.W. 66th St., Bldg. 7, Oklahoma City, OK 73116

Natural attenuation is receiving increased attention as a remedial option for organic components of landfill leachate in aquifers. The availability of electron acceptors and the distribution of microbially mediated redox reactions are important factors for evaluating the efficacy of intrinsic bioremediation in organic-contaminated hydrogeologic environments. In an aquifer contaminated by landfill leachate in Norman, Oklahoma, variable transport rates of volatile organic compounds in the anoxic plume indicate that biodegradation is a key factor in limiting the migration of these compounds. A combined geochemical and microbiological approach was used to delineate the microbially mediated redox processes occurring in the aquifer. The highest rates of sulfate reduction (13.2 micromolar/day) were detected near the water table where sulfate levels were highest (up to 4.6 millimolar). Enrichment of S-34 of dissolved sulfate (ΔS-34 of sulfate was 67–69 per mil) and dissolved hydrogen measurements provided additional support for the importance of sulfate reduction near the water table. Methane was detected in the center of the plume where sulfate was depleted.

Sediment-water incubations under anaerobic conditions demonstrated concomitant sulfate reduction and methanogenesis in sediment from the anoxic portion of the aquifer. Although high concentrations of dissolved ferrous iron were detected throughout the aquifer, and dissolved hydrogen levels indicated iron reduction, the sediment-water incubations showed that iron reduction was active only in sediment collected at the edges of the sulfate-depleted portion of the plume. The microbial incubations combined with geochemical measurements provided a robust identification of areas of in situ sulfate reduction activity and, to a lesser extent, methanogenesis. The results of this study underscore the benefits of conducting microbiological incubations along with measuring chemical concentrations in situ, when evaluating biogeochemical processes that occur in contaminated subsurface environments such as landfill leachate-contaminated aquifers.

Reprinted as published in the Geological Society of America *2000 Abstracts with Programs*, v. 32, no. 7, p. A-127.

Geomorphology and Sedimentology of the Canadian River Floodplain Adjacent to the Norman City Landfill, Oklahoma

KELLI L. COLLINS, BARBARA E. PICKUP, APRIL L. GILLILAN, STANLEY T. PAXTON, and *RICHARD A. MARSTON*, School of Geology, Oklahoma State University, Stillwater, OK 74078; and *SCOTT CHRISTENSON*, U.S. Geological Survey, Water Resources Division, 202 N.W. 66th St., Bldg. 7, Oklahoma City, OK 73116

The Norman Landfill is a closed municipal landfill located on the floodplain of the Canadian River in Norman, Oklahoma. The landfill accepted solid waste from the city between 1922 and 1985, at which time the closed landfill was covered with a vegetated clay cap. The purpose of our project was twofold: (1) determine the location of permeability pathways through which leachate from the Norman Landfill could reach the Canadian River; and (2) establish the geomorphic stability of the Canadian River and floodplain adjacent to the Norman Landfill that affects the mobility of contaminants and susceptibility of the landfill to erosion. We acquired cores and/or conductivity logs for the entire thickness of the floodplain alluvium at over 80 sites. Three-dimensional models of stratigraphy and permeability were developed along with a map of surface sediments. GIS analyses of digitized aerial photos revealed patterns of river migration and floodplain accretion/erosion. The erodability of the Norman Landfill was assessed using field data on cap thickness, compressive strength, and vegetative cover. We have concluded that there is a high probability that leachate will be released to the Canadian River by floodplain erosion. The methods developed in this study will be used to guide investigative procedures for similar landfills around the USA.

Reprinted as published in the Geological Society of America *2000 Abstracts with Programs*, v. 32, no. 7, p. A-286.